ISSN 2730-2695

THAI GEOSCIENCE JOURNAL

THAI GEOSCIENCE JOURNAL

Vol. 4 No. 6 July 2023

Published by
Department of Mineral Resources
Geological Society of Thailand
Coordinating Committee for Geoscience
Programmes in East and Southeast Asia (CCOP)

Editorial Committee

On the cover

1) Debris Flow Area, Sungai Kupang Debris Flow Geological Hazard *(Amir Mizwan Mohd Akhir* et al., *p.11, fig. 6)*

2) The latest rockslide big event happened in the north part of the Prasat Hin Pan Yod chamber, Khao Yai Island on February 20, 2021(*Sakda Khundee* et al., *p.15, fig. 1)*

THAI GEOSCIENCE JOURNAL

Vol. 4 No. 6
July 2023

Published By
Department of Mineral Resources • Geological Society of Thailand
Coordinating Committee for Geoscience Programmes in East and Southeast Asia (CCOP)

Thai Geoscience Journal website at http://www.dmr.go.th

Thai Geoscience Journal
Vol. 4 No. 6
July 2023
ISSN 2730-2695

LIST OF CONTENTS

Thai Geoscience Journal 4(6), 2023, p. 1-13

ISSN-2730-2695; DOI-10.14456/tgj.2023.3

Debris Flow in Peninsular Malaysia - Case Study on Sungai Kupang Debris Flow, Kedah

Amir Mizwan Mohd Akhir*, Saiful Abdullah, Mohd Farid Abdul Kadir, Abd Rahim Harun, Zamri Ramli, Hisamuddin Termidi

Department of Mineral and Geoscience Malaysia
Corresponding author: amir@jmg.gov.my
Received 26 December 2022; Accepted 15 June 2023.

Abstract

Kampung Iboi and several villages downstream of Sungai Kupang, Baling, Kedah were hit by a debris flow and mud flood on 04 July 2022. The disaster claimed the lives of three people, destroyed 17 houses and affected 3,546 residents with losses estimated at RM25.91 million. The flooding that hit Kampung Iboi had high destructive power became the main cause of death, and the bridge to be washed away with several houses completely destroyed along the route. With the calculated amount of debris dumped along the river channels, from landslides to mud flow area of 7.25 million m^3, the quantity of water capable of transporting debris is estimated at 11.23 million m^3. Considering the area of the sub-basin receiving high intensity rainfall of around 10 km^2, rainfall in mountainous areas is estimated at 290 mm/hour.

Result from site investigation show that the disaster area can be divided into four zones; namely the landslide zone, the debris flow zone, the debris flood zone and the mud flood zone. A total of 59 large (>5000 m^2), medium (1000-5000 m^2) and small (<1000 m^2) landslides were identified with a total landslide mass volume of 276,038 m^3. The landslides zone occurs on slopes with an average angle of 30°-35° in the upstream areas which is covered by secondary forest. In the debris flow zone, material consist of the rock blocks (2.0 m to 5.0 m), tree trunks, sand, silt and mud were deposited forming deposits with a thickness of 3.0 m and a cumulative volume of 2,589,021 m^3. The debris flood zone is characterized by materials such as tree trunks, sand, silt and mud that were deposited in areas which is less than 5º slope. The length of this zone reaches up to 6.0 km with an average thickness of debris of about 1.6 m and a volume of 3,275,467 m^3. Mud flood zone was occurred as far as 5.3 km away from the slope with flood height ranging from 0.2 m to 2 m, covering an area of 150 m to 680 m in width. It is estimated that the flood zone carried about volume of 1,111,178 m^3 consisting mainly of mud and silt. The Debris Flow Geological Hazard Map produced during the investigation has identified three post-disaster management zones, i.e. Destructive Zone, Hazard Zone and Safe Zone.

A team lead by Department of Mineral and Geoscience Malaysia (JMG) consists of experts from various department has been assigned to conduct a forensic study in order to understand the cause and effect of this catastrophic event. Several short-term and long-term mitigation measures have been proposed to address existing disasters and to face the threat of debris flow phenomenon throughout the country in the future. The strategy of reducing the risk of debris flow should be implemented holistically in order to improve more integrated disaster management.

Keywords: Debris Flow, Sungai Kupang, Debris Flow Geological Hazard Map

1. Introduction

The phenomenon of debris flow in Malaysia is one of the most feared events, following the high destructive power possessed along its route. Debris-flows is a natural phenomenon in mountainous and steep natural terrains, well-known as fast-moving landslides which generally occur during periods of heavy rainfall (Ghazali, 2013). They consist of loose soil, rocks, and tree trunks combined with water, forming slurry that flows downslope which can displace boulders, may carry away vehicles, houses, bridge and other objects due to their relatively high density and viscosity down the stream (Jimjali Ahmed, 2020). Records show that the landslide incidents including debris flow brought significant losses to the country resulting in more than 500 deaths (since 1961) and property destruction estimated at RM3 billion (1973 - 2007) and it is expected to increase by up to 17 billion in the next 25 years if no long-term mitigation plans are taken. The country is also facing various challenges due to the climate crisis which is changing the pattern, frequency and intensity of rainfall. Climate change has caused a cascading effect which involve landslides, debris flows, debris floods and mud floods. The disaster have recorded a high mortality rate in Malaysia with the total of 442 deaths in 27 years (1995-2022) and economic losses estimated at almost RM904.2 million. Apart from extreme weather, anthropogenic factors such as changes in land use for agricultural development in high degree slope areas can increase systemic risk rates, emerging hazards and geological disasters.

The earliest record in Malaysia explaining debris flow incident is at KM 38.6 Karak Highway-Genting Sempah, Selangor and Pahang on 30 June 1995 which claimed 20 lives, rammed and swept away by a stream of debris more than 50 m from the road to Genting Sempah. The largest debris flow occured on 26 December 1996 in Sungai Keningau, Sabah, killing 300 people and 5,000 houses along the river. The tragedy is well-known as Greg Typhoon due to heavy rains that cause the landslide and debris flow triggered by the tail of Greg Typhoon which began to lose energy when it reached the coast of Sabah. In the same year, another debris flow incident occurred on 26 August 1996 in Pos Dipang, Perak claimed 44 lives (Komoo, 1997). Three (3) large-scale landslides occurred on the steep slopes of high ridges triggered by heavy rains and the debris flowing into the river, destroyed more than 20 houses of Orang Asli. Since then, more than 25 debris flow incidents have been recorded including the Gunung Pulai Debris Flow, Johor on 28 December 2001 (killing 5 lives), Ruan Changkul Debris Flow, Sarawak on 28 January 2002 (killing 16 lives), Sungai Ruil Debris Flow, Pahang on 07 August 2011 (killing 7 lives), Sungai Lubok Panjang Debris Flow on 18 August 2021 (killing 6 lives), Sungai Lui Debris Flow, Selangor on 18 December 2021 (killing 3 lives), Sungai Telemung Debris Flow on 18 December 2021, killing 8 lives) and Sungai Kupang Debris Flow on 04 July 2022 (killing 3 lives). The complete list and its distribution are shown in Table 1.

Department of Mineral and Geoscience Malaysia (JMG) is taking the lead in the investigation of debris flow in Malaysia, has conducted forensic studies with the help and support by experts from various government agencies to find the cause of the incident and produce a comprehensive report to formulate recovery and mitigation plans for the benefit of the affected communities.

2. Case Study Area

Kampung Iboi, a Malay traditional village and several villages downstream which are located on the banks of Sungai Kupang, Baling, Kedah were hit by the debris and mud flood on 04 July 2022. The disaster claimed 3 people, destroyed 17 houses and affected 3,546 with losses estimated at RM 25.91 million. The disaster with a high destructive power is the main cause of death and destruction of many infrastructure (Fig. 1). This incident happened very quickly, starting around 4 pm and the flood receded only after the next few hours. The debris flow and flood in Kampung Iboi was caused by a combination of several geological processes in the upstream area of Sungai Kupang. Heavy rains have triggered

Table 1. List of Debris Flow Incidents in Malaysia

No	Date	Incident Name and Location	No of Deaths	Type of Disaster
1	30 June 1995	Debris Flow at KM 38.6 Lebuh raya Kuala Lumpur–Karak, Genting Sempah, Selangor	20	Debris flow
2	29 August 1996	Mud Flood at Kampung Orang Asli, Pos Dipang, Kampar, Perak	44	Debris flow, debris flood and mud flood
3	26 Dec 1996	Tropical Typhoon Greg at Keningau, Sabah	300	Debris flow, debris flood and mud flood
4	4 Jan 2000	Landslide at Cameron Highland, Pahang	6	Debris flow
5	22 Sep 2001	Landslide at Kampung Chinchin, Gombak, Selangor	1	Debris flow
6	28 Dis 2001	Debris Flow at Sungai Pulai, Gunung Pulai, Johor	5	Debris flow
7	28 Jan 2002	Landslide at Ruan Changkul, Simunjan, Sarawak	16	Debris flow
8	8 Nov 2002	Landslide at Taman Hillview, Hulu Kelang, Selangor	8	Debris flow
9	10 Nov 2003	Landslide at Seksyen 23.3 ke Seksyen 24.1, Kuala Kubu Baru, Selangor	0	Debris flow
10	2 Nov 2004	Debris Flow at KM 52.4, Lentang, Lebuhraya Kuala Lumpur–Karak, Pahang	0	Debris flow
11	10 Nov 2004	Landslide at KM 302, Lebuhraya Utara Selatan, Gunung Tempurung, Perak	0	Debris flow
12	12 Nov 2004	Landslide at Taman Harmonis, Gombak, Selangor	1	Debris flow
13	12 Apr 2005	Landslide at KM 33, Simpang Pulai, Cameron Highland, Pahang	0	Debris flow
14	15 Nov 2007	Landslide at KM 4 ke KM 5, Gap, Jalan Fraser's Hill, Pahang	0	Debris flow
15	15 Jan 2008	Debris Flow at Jalan Fraser's Hill, Pahang	0	Debris flow
16	3 Jan 2009	Landslide at Seksyen 62.4, Jalan Lojing-Gua Musang, Kelantan	0	Debris flow
17	7 Ogos 2011	Landslide at Kampung Orang Asli, Sungai Ruil, Cameron Highlands, Pahang	7	Debris flow and debris flood
18	23 Okt 2013	Landslide at Lembah Bertam, Cameron Highland, Pahang	1	Debris flow
19	5 Nov 2014	KM 28, Jalan Tamparuli, Ranau, Sabah	0	Debris flow
20	11 Jun 2015	Debris Flow at Jalan Fraser Hill's, Pahang	0	Debris flow
21	18 May 2015	Landslide at KM 38.80, Jalan Penampang Tambunan Dongongan, Sabah	0	Debris flow
22	15 Jun 2015	Debris Flow at Sungai Mesilau, Kundasang, Sabah	0	Debris flow
23	23 Ogos 2015	Debris Flow at Sungai Kedamaian dan Panataran, Kota Belud, Sabah	0	Debris flow
24	18 Ogos 2021	Flash Flood, Gunung Jerai, Yan, Kedah	5	Debris flow, debris flood and mud flood
25	18 Dis 2021	Flood di Bentong, Pahang, Hulu Langat, Selangor dan Negeri Sembilan	23	Debris flow, debris flood and mud flood
26	27 Feb 2022	Debris Flow at Empangan Kenyir, Terengganu		Debris flow
27	4 Jul 2022	Debris Flood at Sungai Kupang, Kedah	3	Debris flow, debris flood and mud flood
Total of Deaths			442	

dozens of landslides in the ridges and steep slopes. Material with high water saturation formed debris flow and consequently turned into a debris flood as the water content increased. The Kampung Iboi Bridge became a 'temporary dam' which caused the debris flood in the downstream area when it burst. After the debris was deposited, the leftover materials mainly consist of mud and silt formed the mud flood further downstream.

Fig. 1: Photo of Kampung Iboi, Sungai Kupang, Kedah (the most affected area)

3. Geology and Geomorphology

The entire Sungai Kupang Basin is underlain by three main rock units, namely Inas Granite in the upstream part of the basin with high topography (ranging from 200 m to more than 1450 m), Semanggol Formation in the middle and Kroh Formation which forms the low and undulating hills at the very downstream (Fig. 2). The Inas Granite in the upstream covers almost 70% of the rock distribution in the Sungai Kupang Basin area. The granite consists of medium- to coarse--grained porphyritic granite formed by quartz, feldspar and biotite minerals. The Semanggol Formation, which consists of laminated black mudstone and sandstone, forms the lowland that underlies almost 25% of the Sungai Kupang Basin area. This formation is separated from the granite by a major fault know as Bok Bak Fault. This fault has formed a clear topographic or slope change from steep in the granite area to very gentle land in Semanggol Formation. The Kroh Formation is exposed further downstream of the river which is occupies about 5% the basin area. Its consists of black shale, calcareous shale and limestone. Some of these rocks have been metamorphosed into slate, phyllite and hornfels that contact with granitic rocks.

The Bok Bak Fault is oriented in a direction of northwest-southeast (NW-SE) affects the downstream direction of Sungai Kupang. It also produced a shear zone that created a weak zone between the granitic and sedimentary rocks, producing minor faults (weak zones on the slope) as well as influencing the geomorphology of the Sungai Kupang catchment area.

The geomorphology of the Sungai Kupang Basin is dominated by the mountainous landscape of the Bintang Range which forms Mount Inas with a height of 1454 m and Mount Bok Bak with a height of 1199 m. The geomorphological characteristics of the

upstream to low-lying area are controlled by the underlying rock and lithological units. Between the peaks and the lowlands, there are river channel with V-shaped that became the transport zones of debris. The dendritic drainage pattern upstream form four (4) sub-basins that eventually merge with the main river forming the Sungai Kupang Basin (Fig. 3).

4. Rainfall Distribution

In Malaysia most rain gauges are installed in lowland areas. In the Sungai Kupang Basin, only one (1) rain gauge station is installed in Kampung Iboi. On July 4, 2022, the rainfall reading in Kampung Iboi was around 36 mm within 3 hours. The rainfall intensity at gauging station is considered small and does not allow such a phenomenon to occur unless there are other influences such as heavy rainfall happened in the highlands of Mount Inas where there is no rain gauge to record it.

Based on the amount of debris dumped along the river channels, from landslides to mud flow area which is about 7.25 million m^3, the quantity of water capable of transporting debris is estimated at 11.23 million m^3. Considering the area of the sub-basin that receives high intensity rainfall of around 10 km^2, rainfall in mountainous areas is estimated at 290 mm/hour (KeTSA, 2022). Using the United State Geological Survey (USGS) Rainfall Calculating based on a sub-basin area of 10 km^2, rainfall for the same amount of debris is 200 mm/hour. Based on the estimated, the rainfall during landslides and debris flow is at least 200 mm/hour for 4 hours in Sungai Kupang Basin for the day of incident.

5. Erosion and Siltation

Based on satellite images released by the Malaysian Space Agency (MySA), 813 hectares in Compartment 8 were deforested in 2019, this has led to an erosion rate of 743,895 metric ton/year (Fig.4.A). For the first 6 months of 2022, the area has been deforested and turned into agriculture land with an area of 980 hectares and the annual erosion rate is 57,330 metric ton (Fig.4.B). The rate of erosion used for the calculation of the load rate that goes into the river channels based on soil erosion and siltation studies by Gharibreza et al. (2013). In summary, within 3 years from 2019 to 2022, the rate of erosion that goes into the river channels in Sungai Kupang Basin is estimated at 1,011,006 metric ton as shown in Table 2.

6. Site Investigation

Site investigation are carried out by walk-over survey along the affected river channels from 16-23 July 2022 and aerial survey conducted on 27 July 2022. Based on the site investigation, the disaster area can be divided into four zones; namely the landslide zone, the debris flow zone, the debris flood zone and the mud flood zone (Fig. 5).

a) Landslide Zone

A total of 59 large (>5000 m^2), medium (1000-5000 m^2) and small (<1000 m^2) landslides were identified with a total landslide mass volume of 276,038 m^3. The landslides occurred at an average angle of 30°-35° at upstream areas in secondary forest. Based on Varnes (1978) classification, landslides were dominated by the translational landslide (slides failure). The landslide is 3-5 m wide, 5-10 m long and is classified as shallow (depth of 1.5 m – 5 m). The landslide zone is 0.3 km long. Most landslides occur on the soil layer of the weathered granite, and the shallow sliding on the plane between weathering soil and fresh rocks.

b) Debris Flow Zone

Field surveys, satellite imagery and UAV analysis showing the debris flow in four (4) sub-basins sizing from 20 m width, flowing to the main stream of Sungai Kupang with an average size of 40 m. The length of debris flow is following the length of the river, and the longest debris flow is reaches to 5 km. The debris flow with thickness of 3.0 m transports the rock blocks (2.0 m to 5.0 m in diameter), tree trunks, sand, silt and mud along the stream with a cumulative volume of 2,589,021 m^3. Suspended silt and mud in the water can be

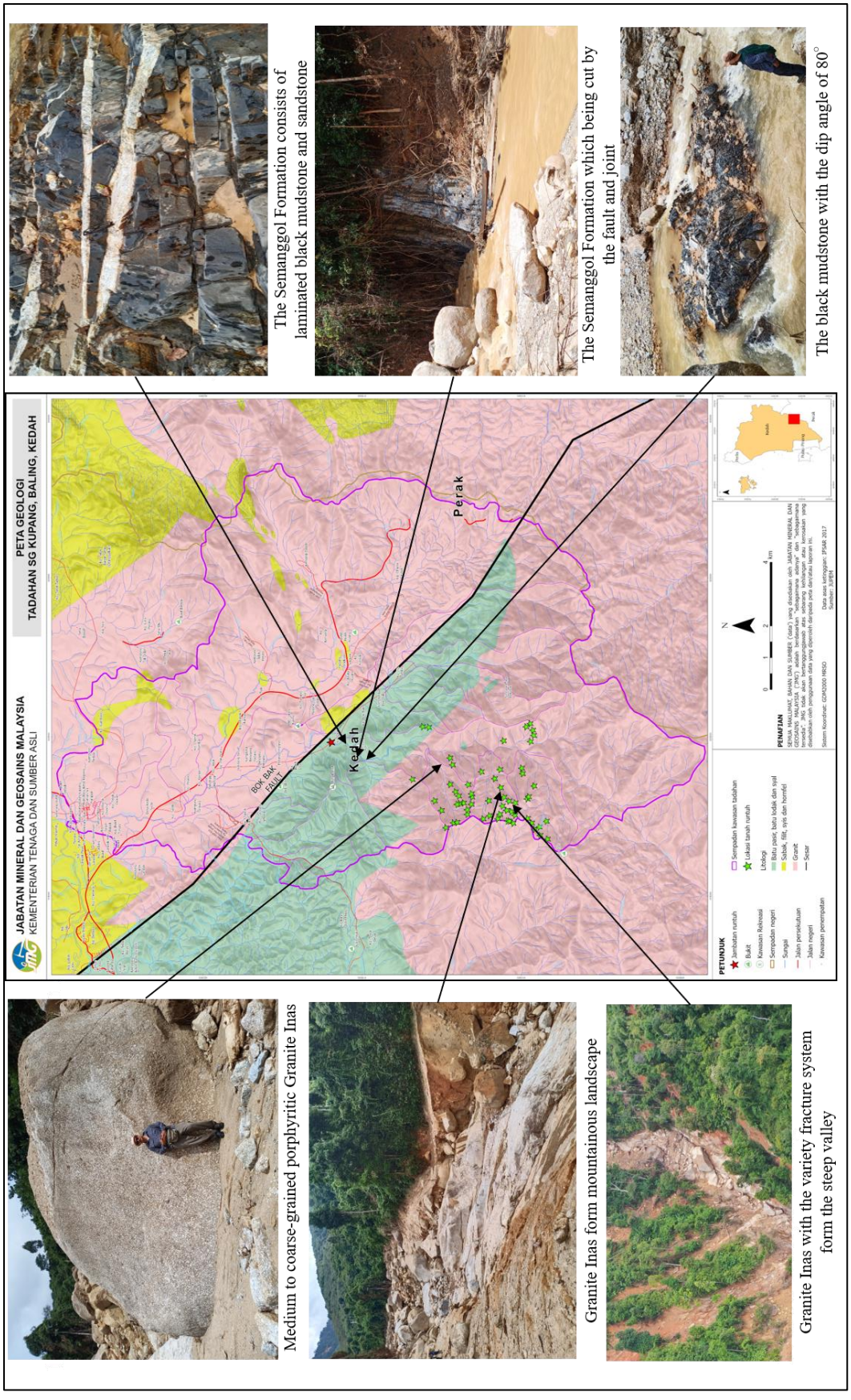

Fig 2: The Geology Map of the Sungai Kupang Basin (Source: JMG, 2022)

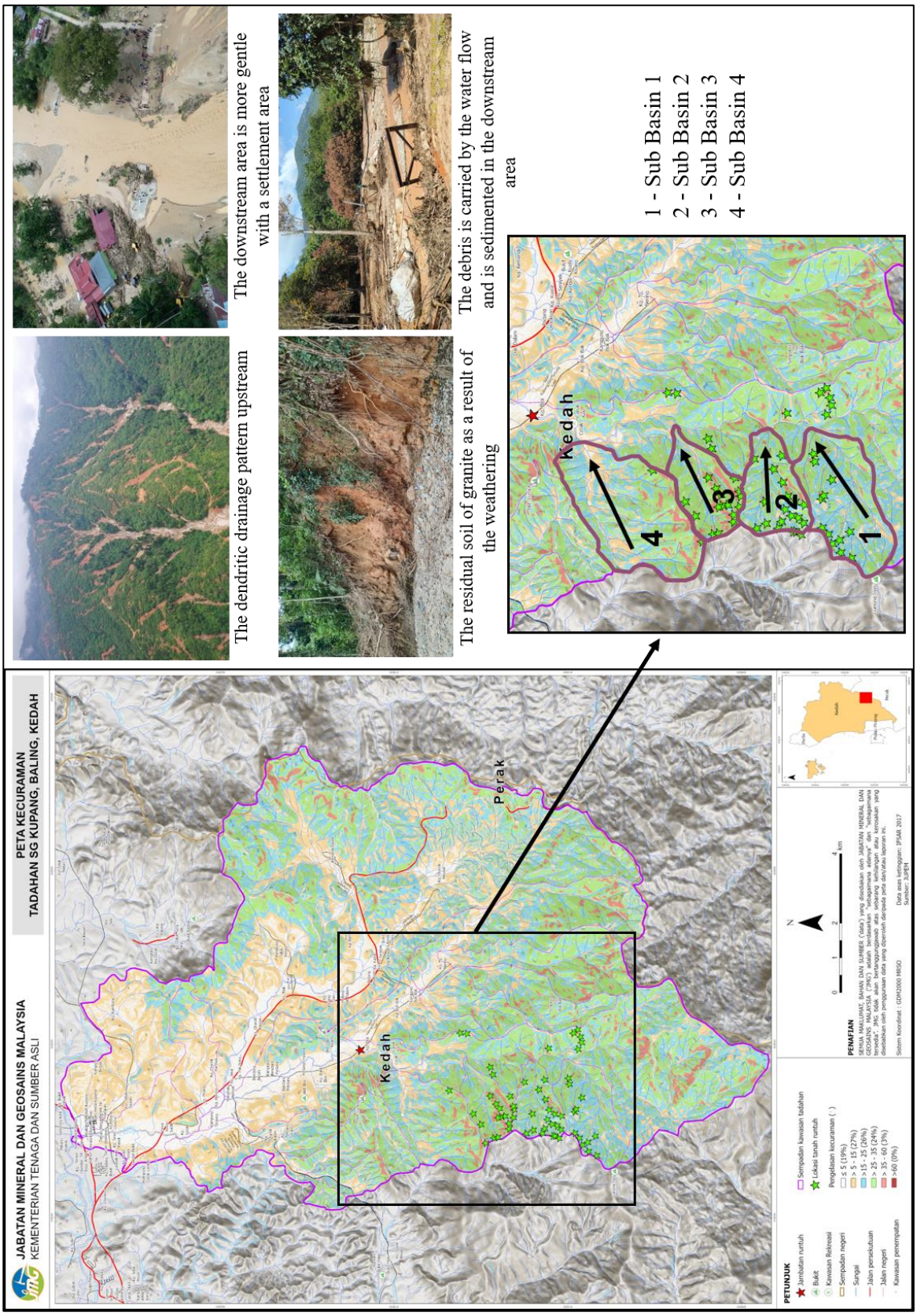

Fig. 3: The Geomorphology Map of the Sungai Kupang Basin (Source: JMG, 2022)

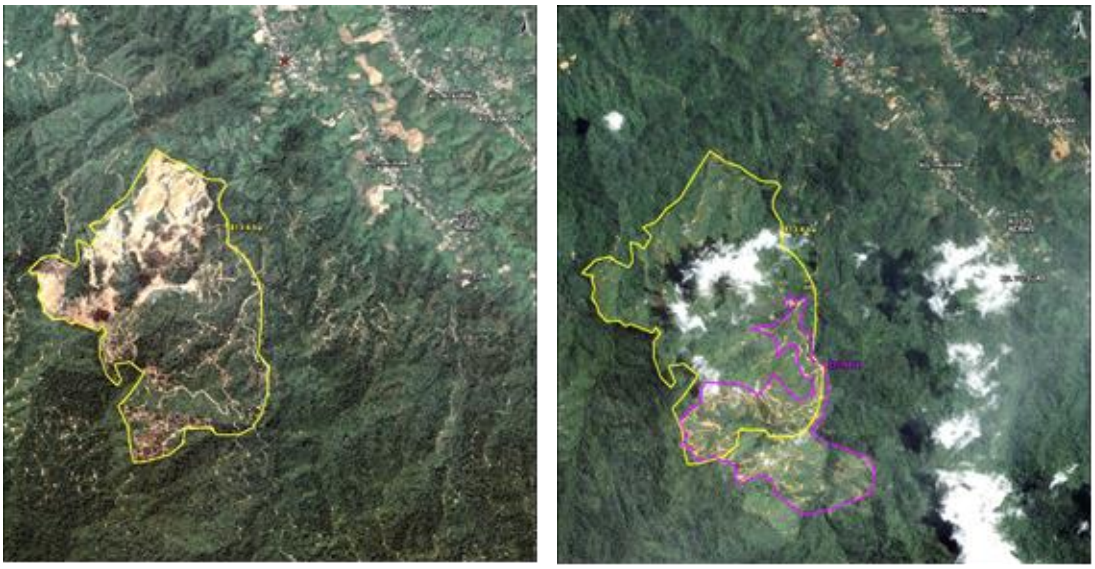

(A) (B)

Fig. 4. (A) Cleared Area (yellow line) in 18 Mac 2019 (813 hectares) (B) Cleared Area (yellow & purple line) in 02 July 2022 (980 hectares) (Source: MySA, 2022)

Table 2. The Erosion and Siltation Rate in Compartment 8 using Gharibreza et al., 2013.

Year	Area (Hectares)	Erosion Rate [Unit – metric ton per hectares annually]	Total [metric ton]
2019	813	915	743,895
2020	813	117	95,121
2021	980	117	114,660
2022 (Jan -Jun)	980	58.5	57,330

transported further downstream. Due to the medium gradient of rivers (15° to 35°), many rock blocks are stranded along the debris flow profile.

c) Debris Flood Zone

As the water content increases and a lot of debris is sedimented, the debris flow turns into a debris flood. The impact of the flooding began at the river mouth of Sungai Celak, about 1.2 km upstream of Kampung Iboi. Field findings show that Kampung Iboi received the main force from the impact of transported debris up to 800 m wide and weakened in the area of Kampung Hangus with a width of 450 m. The debris flood brought a lot of tree trunks, sand, silt and mud. Debris flood zone does not involve many geomorphological mechanisms (the slope angle is less than 5º), reaches up to 6.0 km with an average thickness of 1.6 m and volume of 3,275,467 m^3. Within this zone, a total of 4 bridges located between Lata Celak and Kampung Iboi have collapsed. Apart from that, infrastructure such as roads and some of the residents' houses were destroyed and badly damaged by the impact of debris and overflowing river water.

d) Mud Flood Zone

After the debris containing sand and tree trunks are stranded, the floodwater contains only high volume of silt material. Depending on the height of the water level, mud flood can overflow on the flood plains extensively. The recorded mud flood level ranges from 0.2 m to 2 m with the width ranges from 150 m to 680 m and estimated volume of 1,111,178 m^3. Mud flood zone was detected as far as 5.3 km from Kampung Hangus to Kampung Kuala Kupang and affected 36 villages along Sungai Kupang. The distribution of these zones is very wide and involves damage to public facilities and causes discomfort to the affected residents.

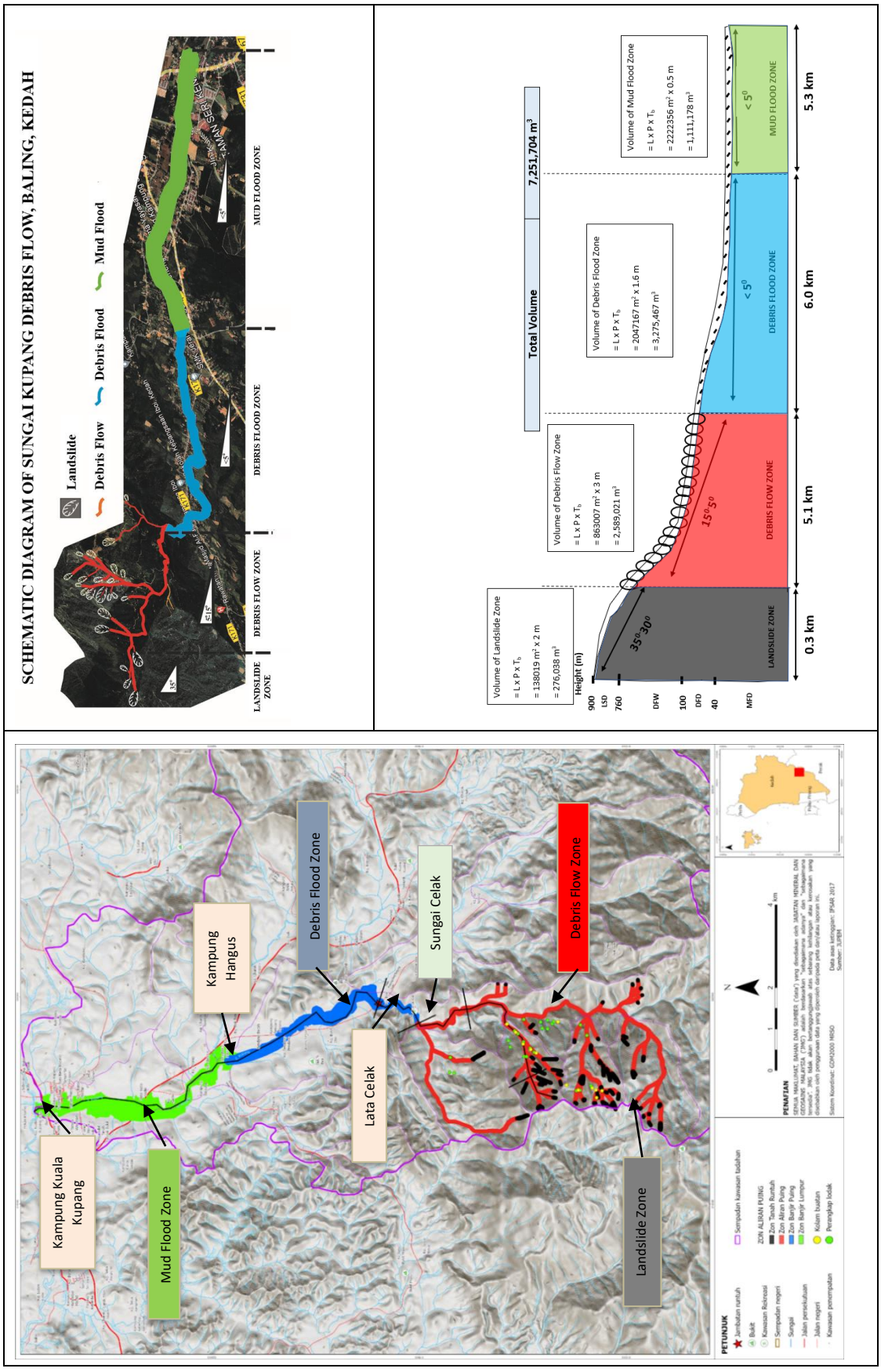

Fig. 5: Sungai Kupang Debris Flow Zone Map (Source: JMG, 2022) (Landslide Zone - Black), (Debris Flow Zone - Red), (Debris Flood Zone - Blue), (Mud Flood Zone - Green)

7. Debris Flow Geological Hazard Map

Based on field investigations and geomorphological analysis, a Debris Flow Geological Hazard Map is provided. This map is intended to be used as a post-disaster development planning guide in areas where the debris flow disaster has occurred. This hazard map takes an approach which the disasters that have occurred can recur in the future and the rebuilding process should take the current experience into account. For this hazard map, three post-disaster management zones were introduced, namely the Destroy Zone, the Hazard Zone and the Safe Zone (Fig. 6).

a) Destructive Zone

The Destructive Zone involves areas affected by landslides, debris flows and debris flood. Based on current surveys, any infrastructure in this zone can be destroyed if the repetitive debris flow occurs at the same intensity or more. Houses can be destroyed, while residents who are inside houses will be difficult to save. For disaster management purposes, all elements of infrastructure remain unsuitable for development in this zone and should be placed as a buffer zone, agricultural area or recreation site with an appropriate disaster early warning system.

b) Hazard Zone

The Hazard Zone involves areas affected by mud flood. Based on field surveys, most of these areas experienced mud flood at the level of waist-down (2 to 3 feet). Most losses involve property damage and discomfort, without building destruction or death. This zone can still be occupied or build permanent infrastructure, if risk factors and mitigation are considered in planning and construction.

c) Safe Zone

The Safe Zone in the basin is an area that is not affected with the debris flow at all and the repeating impending debris flow. This zone is suitable if reconstruction activities need to be carried out, in particular for the evacuation of houses or settlements that are severely affected by the debris flow. Safe zone is suitable area for the construction of schools, health centres and public buildings.

8. Mitigation

The investigation team has recommended short-term and long-term actions that can be implemented as mitigation measures to address existing disasters and to face the threat of debris flow phenomenon throughout the country in the future. Ministries, responder and technical agencies as well as local authorities should arrange the proposed work action based on recommended short-term action (within 2 years) and long-term action (within 5 years).

a) Short Term Action

i detail debris flow mapping within 6 months after the incident, collecting data for follow-up planning to reduce risks to local communities.

ii installation of early warning system including automatic rain gauge in real time. Rainfall information is crucial as the main 'early warning system' to reduce the risk of landslides, debris flows, debris floods or flash floods.

iii evacuation of residents from the Destroy Zone and Hazard Zone to a safe area. During these few months, the river water will remain murky, while flooding will be easier to happen due to shallow river conditions.

iv river deepening and continuous cleaning of debris to reduce the risk of post-disaster flooding.

v planting a deep rooting trees, shrubs, and ground cover plants in open areas to reduce the rate of erosion.

vi implementation of Community Empowerment Programs (C.E.P.) against the threat of landslides, debris flows and debris floods.

vii organising engagement sessions and geological hazard forums in Malaysia.

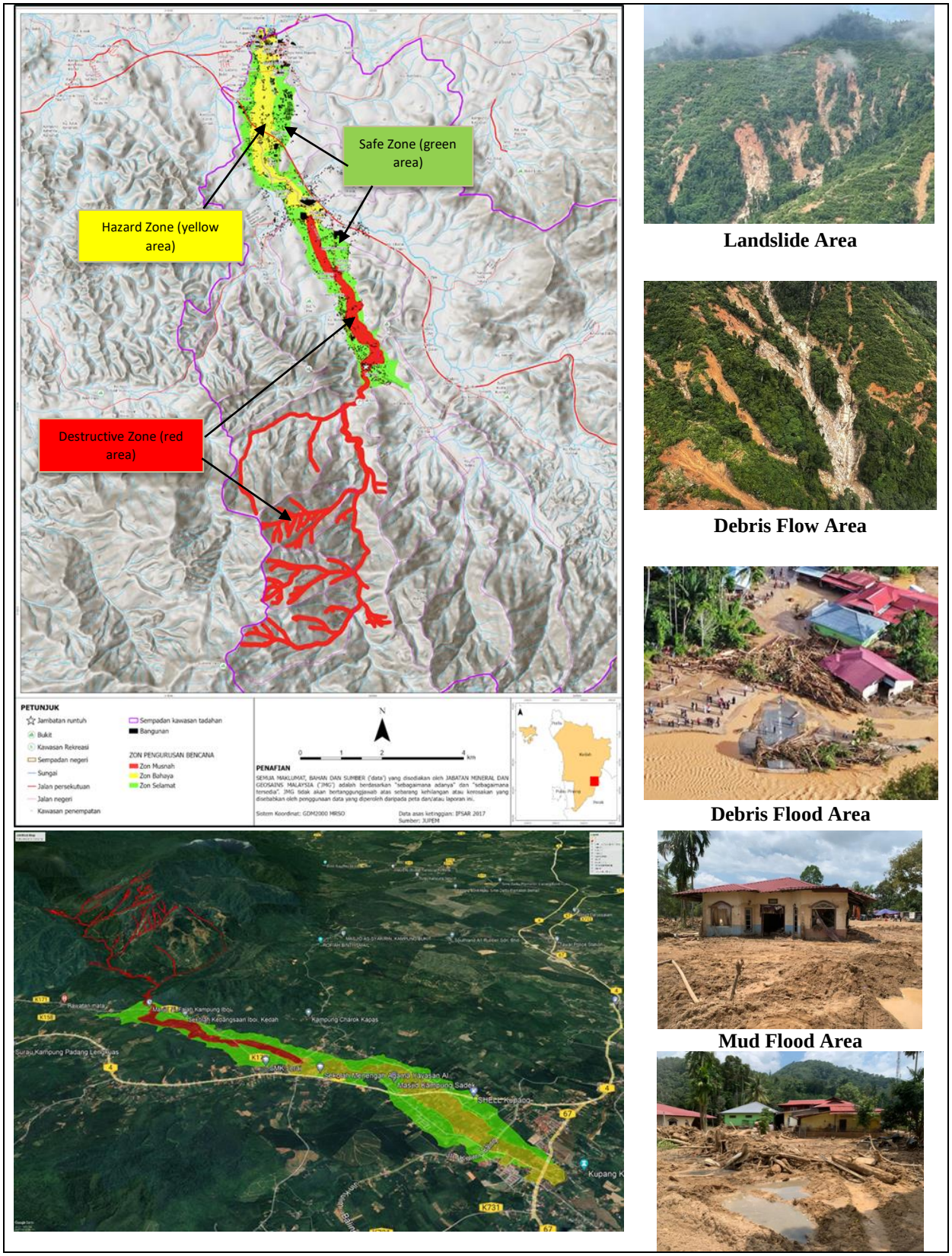

Fig. 6: Sungai Kupang Debris Flow Geological Hazard Map (Source: JMG, 2022) (Destructive Zone - Red), (Hazard Zone - Yellow), (Safe Zone - Green)

b) Long Term Action

i establishment of the National Geological Hazard Research Centre under the Department of Mineral and Geoscience Malaysia (JMG) as a geological hazard information reference centre to conduct forensic studies of geological hazard and strengthen the forecasting, monitoring and warning of national disasters.

ii initiation of the Debris Flow Risk Sub-Basin Mapping Program which use to map the hazard risk forecasts and conduct detailed studies of high-risk sub-basins.

iii the establishment of a geological hazard early warning systems network in the mountainous areas related to geological hazard and managed by the National Geological Hazard Research Centre to strengthen the geological hazard communication and effective announcements.

iv implementation of geological hazard risk mitigation based on structure for debris traps and various functions such as domestic and agricultural water resources, micro-hydro energy, eco-forest parks as well as recreational sites.

v empowerment strategic plan of the Integrated River Basin Management (IRBM) by introducing additional policies for Geological Hazard Management in Basin.

5. Conclusions

The debris flood is a rare event in a sub-basin, occurring when the water content increases and the mechanism of the flow of debris then turns into a debris flood. Debris flow and debris flood is not a common flood, but rather part of a geomorphological process that transports various types of debris material as a result of landslides and debris flows at the highland terrain to the downhill or valley area. It can result in loss of life, damage to infrastructure and destruction of property as well as impact discomfort to the affected communities.

The debris flow events have occurred more than 26 times since 1995 and claimed 442 lives with losses estimated at almost RM904.2 million. The debris flood in the Sungai Kupang Basin which happened on 4 July 2022 in Baling District, Kedah has affected 968 residential premises in 38 villages, resulting in 3 deaths, damage to 35 public infrastructure and have a double impact on survival and business due to damage to agricultural areas, animal farms, and affecting the tourism activities.

Therefore, the strategy of reducing the risk of debris flow should be implemented holistically in order to improve more integrated disaster management. This study is an integrated report based on several technical information of various departments and agencies. This report has recommended short-term and long-term actions that can be implemented as mitigation measures to address existing events and to counter the threat of debris flow across the country in the future.

References

Gharibreza, M., Yusoff, I., Raj, J.K., Othman, Z., Zakaria, W., Tahir, W.M., & Ashraf, M.A. (2013). Land use changes and soil redistribution estimation using 137Cs in the tropical Bera Lake catchment, Malaysia, *Soil and Tillage Research, 131*, 1-10.

Ghazali, M.A. (2013). The Engineering Geology of Debris-flow at Igneous Areas in Peninsular Malaysia. Dissertation, Universiti Kebangsaan Malaysia.

Jabatan Mineral dan Geosains Malaysia, (2022). Bencana Geologi Aliran-Banjir Puing 2022 Sungai Kupang, Kedah.

Jabatan Mineral dan Geosains Malaysia, (2021). Garis Panduan Kajian Forensik dan Pemetaan Geologi Kejuruteraan Aliran Puing di Malaysia, JMG.GP.32

Jabatan Mineral dan Geosains Malaysia & Department of Mineral Resources, Thailand, (2010). Geology of the Pengkalan Hulu-Betong Transect Area Along the Malaysia-Thailand Border.

Jimjali Ahmed, Mohd Raihan Taha, Mohd Anuri Ghazali, Che Hassandi Abdullah and Senro Kuraoka. (2022). Debris-Flows in Peninsular Malaysia: Topography, Geology, Mechanism and Sediment Discharge. *ARPN Journal of Engineering and Applied Sciences*, *15(2)*, 270-283.

Kementerian Tenaga dan Sumber Asli, (2022). Laporan Kajian Bencana Geologi Banjir Puing 2022 di Sungai Kupang, Kedah.

Komoo, I. (1997). Slope failure disasters - a Malaysian predicament, Engineering geology and the environment. *Proc. symposium, Athens*. *1*, 777-781.

Malaysian Space Agency, (2022). Satellite Image of Sungai Kupang Area. Image from 2019 to 2022.

Varnes, D.J. (1978). Slope Movement Types and Processes. *National Academy of Sciences*, 12-33.

Thai Geoscience Journal 4(6), 2023, p. 14-35

ISSN-2730-2695; DOI-10.14456/tgj.2023.4

Rock Failure Assessment on Paleo-Collapse in Case of the Prasat Hin Pan Yod tourist site, Satun Geopark, Thailand

Sakda Khundee, Sarinthip Kukham, Saowaphap Uthairat, Visuttipong Kererattanasathian, Kittikorn Tima and Tanawat Rakhangkul

Environmental Geology Division, Department of Mineral Resources (DMR), Bangkok, Thailand
**Corresponding author: geol.envi@gmail.com*
Received 26 December 2022; Accepted 9 June 2023.

Abstract

Rockfall and rockslide incidents are currently severe geohazards affecting marine tourism in Thailand. Lately, some tourist sites, located both in the Gulf of Thailand and the Andaman Sea, were prohibited to access. Prasat Hin Pan Yod, the study area developed from a paleo-collapse sinkhole on Khao Yai Island of Satun province, is now confronting unsafe caused by rockfall and rockslide hazards as well. The study applied the integration of simple multi-criteria in GIS, traditional stereographic projection analysis, and Slope Mass Rating (SMR) to determine the rock mass instability of limestones and to find a safe route entrancing the Prasat Hin Pan Yod tourist site. Various discontinuities on the outcrop slopes relating to geomorphological features such as sea cliff, sea cave, and a former broken block of the rockslide were investigated and assessed the rock mass stability.

The study result shows that the dominant wedge failure of rockfall can occur in many spots of the Prasat Hin Pan Yod tourist site. Small pieces of broken limestone hanging on high spots and also filling in rock niches are often found during the field investigation. Rock fragments splitting off the rock face may fall away whenever it is triggered by heavy rain or ground shaking. Direct toppling failure is the comparative subordinate of the rockfall hazard. Its negative impact is similar to wedge failure and difficult to perform risk management as well. Planar failure and toppling failure seem to be low scores and rarely occur the two big severe events happened from that failure modes and revealed obvious field evidence of broken blocks. The precedent event was caused by toppling failure and the latest, February 20, 2021, was originated by planar failure. The previous route getting through the Prasat Hin Pan Yod chamber is not suitable now. Depending on the high SMR score and a few joint intersections causing the geohazard, a narrow strait located between the former broken block and sea cliff is determined as the new safe route for tourists. Moreover, Kayaks should be adopted to use for moving through the narrow strait and permitted for in and out. The tourist numbers visiting the site should be controlled. A Helmet is suggested for more safety as it can protect the tourists from the hanging rock falling from high places.

Keywords: RMR, SMR, Prasat Hin Pan Yod, Satun, Rock failure, Rockslide, Rockfall

1. Introduction

Rockfall and rockslide incidents have more frequently occurred in marine attractions in Thailand. Especially, during the southwest monsoon that affected the peninsular region. It causes the base rocks in southern Thailand which are dominant carbonate-rich rocks (ex. limestone, dolomite, and gypsum) that are easy to weather and erosion, so the karst topography is generally formed in this area. Most karst features are formed along with weaknesses in the rock mass, such as faults, joints, fractures, and bedding planes, that karst features decrease rock stability and lead to cause geohazard. Prasat Hin Pan Yod is one of the famous coastal karst landforms in Thailand. The rockfall incident happened here on February 20, 2021, occurred in the north part of the Prasat Hin Pan Yod chamber, Khao Yai Island (Fig. 1). Fortunately, this incident did not cause people to die or be injured. However, spectacular karst morphology has been turned to be a dangerous area.

Tourists and locals were not allowed to visit that place. People in Satun provincial area were indigent due to the loss of tourism revenue. The aims of this study are to assess the anticipated failure of rockfall and rockslide and to find new comparatively safe routes through the Prasat Hin Pan Yod tourist site.

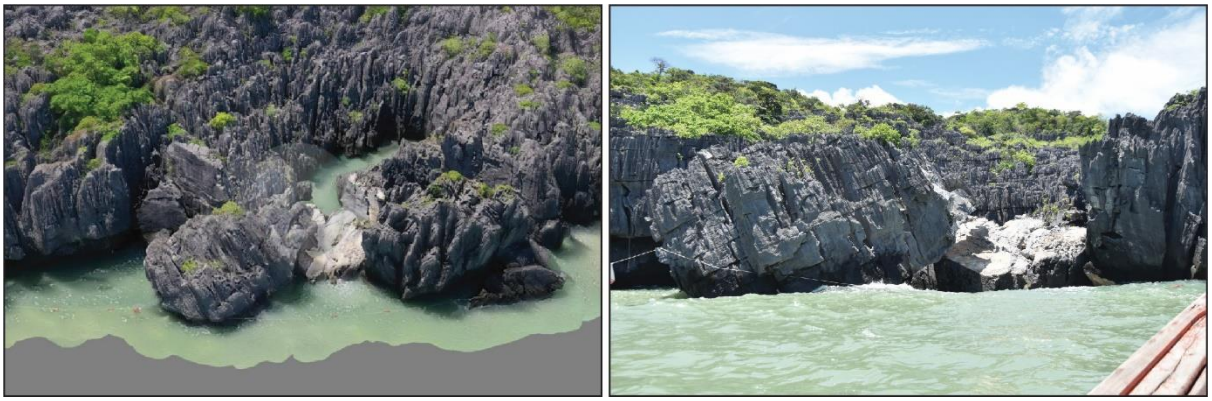

Fig. 1: The latest rockslide big event happened in the north part of the Prasat Hin Pan Yod chamber, Khao Yai Island on February 20, 2021

2. Study area

The Prasat Hin Pan Yod tourist site is located in the north part of Khao Yai Island which is a limestone island in the Andaman Sea, La-Ngu district, Satun province, south of Thailand. Prasat Hin Pan Yod is one of geosites within Satun Geopark which is the first UNESCO Global Geopark in Thailand. The Satun Geopark was endorsed by the UNESCO Executive Board on April 17, 2018. The Geopark covers four districts: Thung Wa, La-Ngu, Manang, and a part of Mueang Satun, and also consists of two national parks and one wildlife sanctuary. The Global Geopark is established by the concept of sites and landscapes of international geological signi-ficance, which are managed with a holistic concept of protection, education, and sustainable development.

3. Geology and geohazard

Based on the lithological descriptions on the geological map scale 1:50,000 published by Sinsakul (1988) and Tiyapairach (2004), Khao Yai Island is abundantly covered by carbonate rocks, which can be classified into strati-graphically lower and upper parts. The lower part is medium to thick bedded dolomitic limestone with partly brown mudstone and the upper part is thicker to massive bedded. Locally, the northern part of Khao Yai Island, where the Prasat Hin Pan Yod chamber is located, mainly consists of dark grey argillaceous limestone and stromatolitic limestone with dominant fossils. Some fossils are occasionally found on the planar failure that is sub-parallel limestone to the bedding plane. Wongvanish (1990) and Meesook (2014) correlated the rocks in this area to the Lae Tong Formation of the Thung Song Group. Their depositional environment is interpreted as pelagic deeper water during the Ordovician period. Thepju et al. (2017) classified onshore karst features in the Satun Geopark into 13 types which are (1) wall karst, (2) stromatolitic karst, (3) pinnacle, (4) cone and tower, (5) knob, (6) Karren or lapies, (7) stone forest, (8) polje, (9) sinkhole or doline, (10) karst spring or karst seepage, (11) karst waterfall, (12) karst lake, and (13) cave. These features are mostly exokarst-subaerial occurring in the Lae Tong Formation and the Rung Nok Formation of the Ordovician Thung Song Group. The Lae Tong Formation is character-ized by thin-bedded argillaceous limestone and interbedded with pinkish-brown shale at the lower sequence. The Rung Nok Formation, overlying the Lae Tong Formation with a gradual boundary, consists of dark grey to grey limestone, medium to thick-bedded limestone with stromatolitic interbedded with occasional stylolite and massive dolomite.

The Prasat Hin Pan Yod chamber is naturally a paleo-collapse sinkhole. Based on the sinkhole classification presented by Waltham et al. (2005), a collapse sinkhole is a roof collapse happening on unstable limestone beneath, particularly cavernous and high fracturing rock. The sinkhole originated on the hinge zone of a small asymmetry anticline whose fold axis is orientated nearly north-south (NNE-SSW) and gently plunged at 11º in a direction 014 (NNE). Limestone bedding planes have an average dip angle of 25 º in direction 320 (NW) and dip at 15 º in direction 035 (NE). A well-defined bimodal clustering on stereonet shows the dominant strike directions of joint and fracture in limestone rock mass have approximately four directions. The discontinuous plans are trending nearly north (NNW-SSE to NNE-SSW), northwest-southeast (NW-SE), northeast-southwest (NE-SW), and east-west (E-W). Thinner bedded limestones generally show narrower spacing of joints and higher fracture density compares to massive limestones. Due to the southwest monsoon climate and sea process, the erosional karstic surface is well developed on strongly fractured limestone, particularly in the upper part of its succession. According to karstic landforms, the imagination of people when they look at limestone pinnacles exposed on islands it resembles castle-like features with a thousand peaks.

There is a small chamber of the formal sinkhole surrounded by spectacular limestone pinnacles and hides in the sea cliff. Its geometry is a small oval-shaped room with a longest of 20 meters and the shortest distance of 10 meters. The Prasat Hin Pan Yod tourist site locates in the rocky intertidal zone of the island. By the action of currents and waves, sediments and other detrital material have entered the chamber via sea caves and deposited in a low-energy sinkhole hiding a sea cliff. The small beach will be exposed to air for only a short period when low tide. Tourists can enter in sightseeing site from March to mid-May. Coastal massive limestone is no exception of strongly eroded by the action of the sea. Various karst types are generally found in the intertidal zone: notch, cave, cavity, stack, and column. Enlargement of cave size and connected passage networks has been still processed by both dissolution and erosion until the present time and invaded toward limestone chamber or collapse sinkhole. Cave passages lack the strength to span limestone overburden and create unsafety ground conditions for use.

Far from the Prasat Hin Pan Yod to the south direction of 150 meters, another rectangular-shaped formal collapse sinkhole with a long diameter of 150 meters across can be visible on remote sensing images. It has occurred on major joint/fault intersections having strike orientations on the north-south and northeast-southwest. The comparative size is larger than the others on the Google images (Fig. 2). Because that area is shallowed by sediment deposit and covered by dense water grasses, which karstic characteristics can classify as the older age than a sinkhole of the Prasat Hin Pan Yod. According to the karst engineering classification introduced by Waltham and Fookes (2003), the Prasat Hin Pan Yod can categorize as Complex to Extreme Karst. Besides specific lithology and geological structures, rock strength has been degraded by that various karst features leading to severe geohazard occurrence of the rock mass.

Based on the DMR field evidence, the rockslide occurrence may briefly conclude in four parts. First: erosion of fractured and cavernous limestone by sea, due to the location placing at the narrow strait of Khao Yai Island and the other island on the northern side, strong waves and rapid currents can enter cave passages to hit unstable rock columns that partly support cave roof, because of hydraulic power of the waves and compression of air within a confined space provide the fissures in rock mass widen and deepen and lead to having a broken column. Second: as a result of the supporting column is being broken, the loss of rock strengths cannot carry limestone overburden at the upper part. Third: the massive limestone volumes suddenly separated from the weakened sea cliff along major linear faults. Fourth: the upper part slides through rock mass sub-parallel bedding plane / along low angle fault and falls in the north direction into the sea, hiding the traditional entrance of the chamber. The fragment block of the rock-

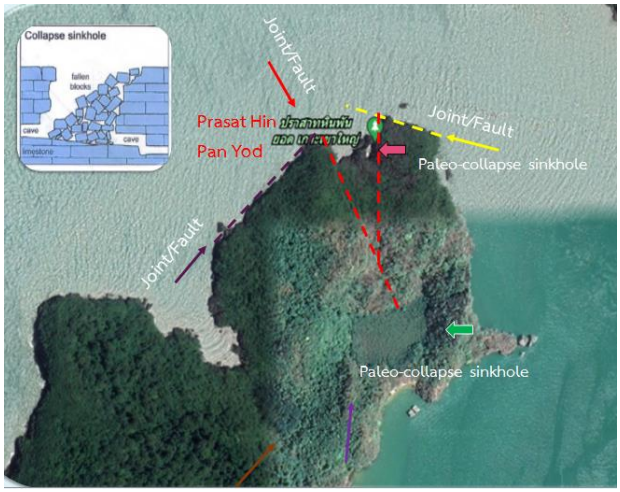

Fig.2: the Prasat Hin Pan Yod chamber showing oval shaped collapse sinkhole that occurred next to an older rectangular shape (Blue arrow)

-slide location is not far from the precedent rock topple. As mentioned above, the paleo-collapse sinkhole at the Prasat Hin Pan Yod can be a recurrence, particularly on the edge of the chamber.

Based on the orthophotos visual inter-pretation, geohazards in the Prasat Hin Pan Yod area have ever occurred at least 2 times: prior to the event on February 20, 2021, there was a precedent topple block sitting nearby the latest rockslide. A huge block of limestone was broken along a major joint/fault and fallen to sea by a toppling failure mechanism. Rockfall and rockslide in the Prasat Hin Pan Yod will happen in the near future.

Sinkhole hazards naturally overspread in the Satun provincial area due to underlying limestone bedrock. The sinkhole potential map of Satun province was hurriedly produced after the big earthquake accompanied by the severe tsunami event in 2004 and the map was firstly published by DMR (2005). The mapping of sinkhole types relating to soil materials, especially dropout sinkholes, was the main task. The potential sinkhole area was delineated by the simple approach of limestone bedrock or mountain proximity. As a consequence, the limestone mountain is generally surrounded by areas of a high potential sinkhole. There have no collapse sinkholes both onshore and offshore represented on the map. To study rock failure, the sinkhole potential area classification must be studied in more detail.

According to Sinsakul et al. (2002), the Satun coastline erosion mapping was initially conducted by the DMR prior to 2002, and the mission of coastal management has been responsible by the Department of Marine and Coastal Resources (DMCR). To monitor shoreline erosion, Khundee et al. (2019) used the Real-Time Kinematic Global Navigation Satellite Systems (RTK-GNSS) method for the beach erosion investigation from the Pak Nam Bara to Ao Noon in the Mu Ko Petra National Park. Beach erosion is the topic study that is more focusing on Thailand. Hard structures are used to reduce the wave action of the sea. Erosion at rocky coasts has rarely been explored by organizations, so data is not adequate to support the study of limestone coast collapse.

Based on the intensity of the Mercalli scale, the seismic hazard map of Thailand published by DMR (2016) is categorized into 5 levels which are I-III, IV, V, VI, and VII. In Satun province, active faults have never been discovered, and the intensity of Satun is I-III which is classified as the lowest level. However, coastal karst terrain can be affected by the Klong Marui fault which is an active strike-slip fault system in southern Thailand. It extends in a northeast-southwest direction from Phuket towards Surat Thani province, and the distance from Satun provincial area to the Klong Marui fault zone is about 290 kilometers.

At coastal karst, tourists often take time in an attractive place without realizing that there is danger from geohazards. Rock failure mode: a planar, wedge, or topple can cause rockslide or rockfall in high fractured limestone of marine karst terrain as the latest rockslide event happened on February 20, 2021. For the safety of tourists, rock mass stability and slope mass stability have to be investigated in the Satun Geopark and Thailand National Park. Moreover, recommendations or guidelines for rock reinforcement are introduced to reduce the opportunity of geohazard risk.

4. Methodology

Six processes were conducted for rock failure assessment (Fig. 3). They are described below.

(1) Making of an orthophoto map obtained from drone flying, lineaments and boundary of limestone rock types can be extracted from the orthophoto by the method of visual interpretation.

(2) Mapping the sinkhole potential area of Satun province.

(3) Mapping preliminary rockfall zonation by the multi-criteria analysis in GIS which the map using for field checking and determining rock stability study in detail.

(4) Collecting the data relating to rock mass discontinuity and clues of former rockfall, and to estimate Rock Mass Rating (RMR) values in field investigation.

(5) Slop Mass Rating (SMR) assessment, the first step is to assess the mode of failure that may be originated rockfall type and to evaluate the stability of outcrop slope due to discontinuity cutting on.

(6) Writing a report, presenting to the provincial office and local government, and giving recommendations for reducing rockfall impacts on tourist sites.

The equipment using in field investigation were geological hammer, compass (Breithaupt), tape measure or ruler, and Schmidt hammer. The Software used for data analysis and displays the imagery maps were Agisoft Metashape, DIPS, and ArcMap.

Field survey was took place at the end of the year 2021 from the coastal limestone outcrop that is considered as having a high potential area of geohazards at paleo-collapse sinkhole and may cause medium to high negative impact. The direct measurement or investigation in the field was composed of four data sets of primary data: photos obtained from drone flying, Rock Mass Rating (RMRb) parameters, slope face orientation of outcrops, and various discontinuity in karstic limestone.

5. Result and discussion

5.1 Orthophoto map obtained from drone flying

The DJI Mavic 2 Pro, a lightweight Unmanned Aerial Vehicles (UAV), was used for achieving the Khao Yai Island image. The traverse line was covered the north part of Khao Yai Island where the Prasat Hin Pan Yod located. According to the time that taking photo was nearly at noon, it allowed dark shadow appeared along the edges of sea cliff, sea cave, and eastern side of the paleo-collapse sinkhole. The images obtained from UAV were totally 1,202 images covering 0.065 square kilometers. For orthophoto making, Agisoft Metashape software was adopted to conduct data processing. The output orthophoto had a Ground Sampling Distance (GSD) of 4.15 centimeters. For data quality control, the horizontal position value (East and North coordination) is quite precise, but its elevation data still have some error. The orthophoto is used for exploring the orientation of rock mass discontinuity and to concentrate on unstable zone due to marine erosion.

5.2 Mapping sinkhole potential area of Satun province

The first sinkhole potential map was published in 2005 by DMR, then it has been updated in 2022 by using GIS. The simple overlay technique of relating factors was utilized for analysis. The five factors adopted for the improvement of sinkhole zoning have consisted of the density of lineament intersection, lineament density, distance to lineament, stream density, and distance to stream. Enhanced sinkhole potential area is classified into five levels which are very low,

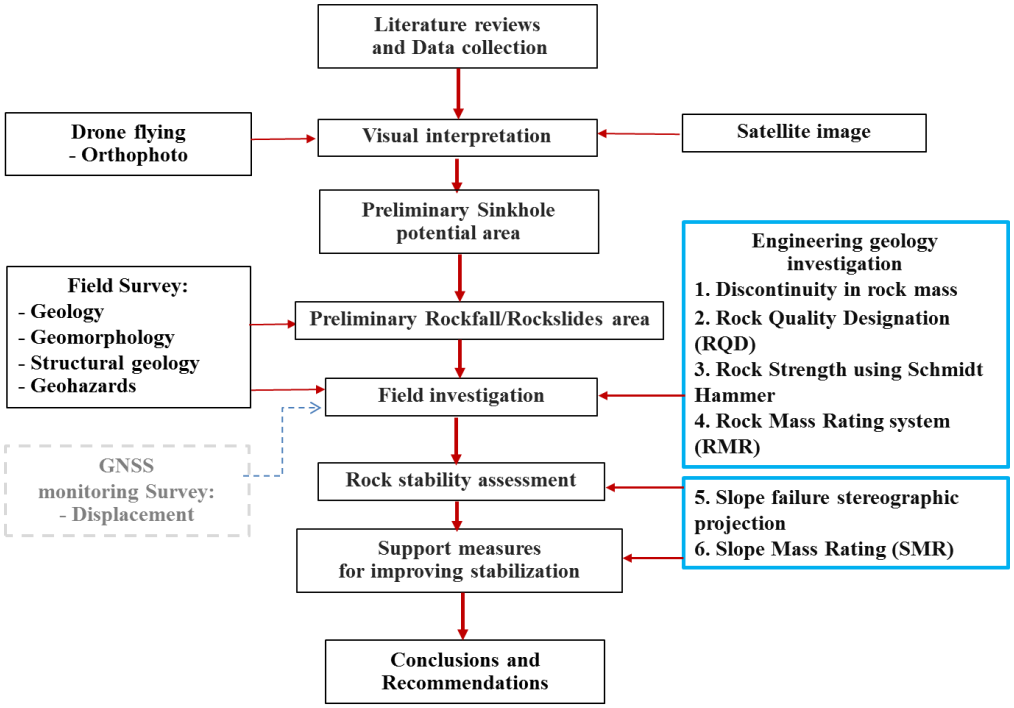

Fig.3: rock failure assessment process

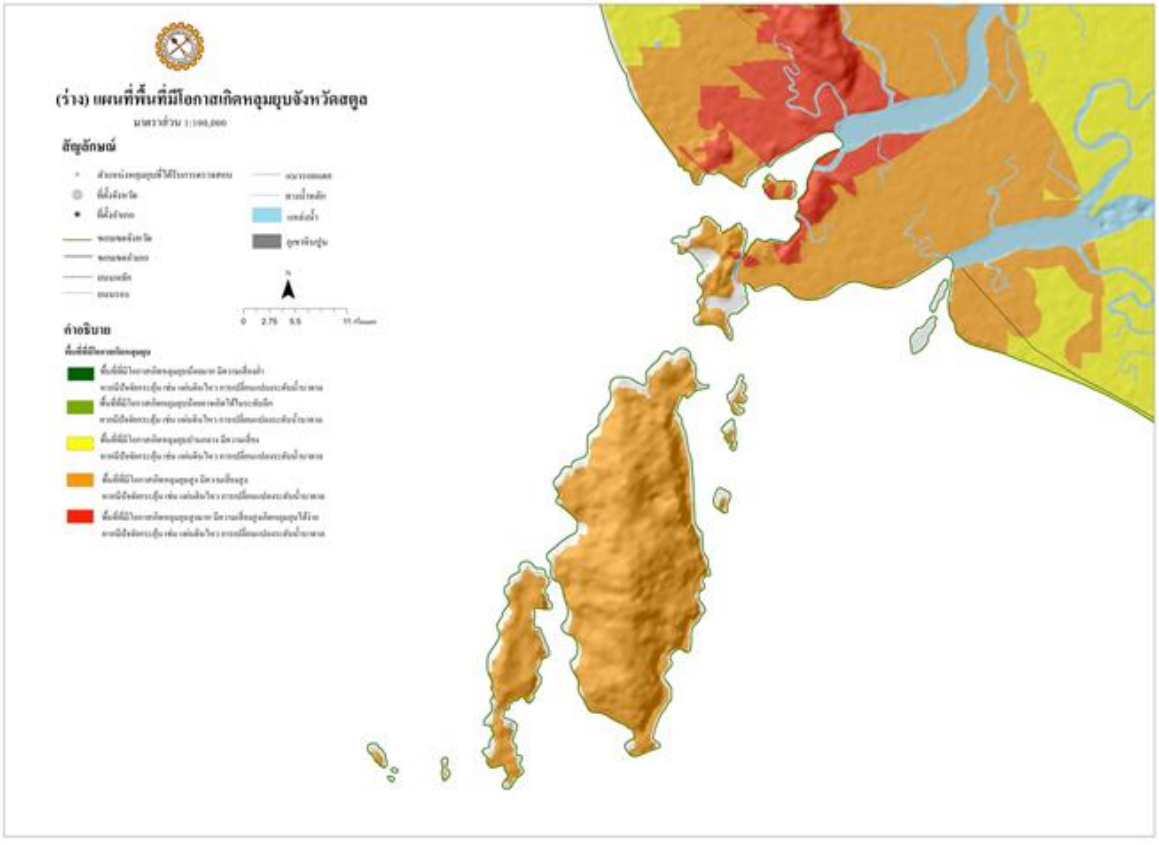

Fig.4: High sinkhole potential covering the Prasat Hin Pan Yod chamber (Black dash rectangular shape) and the overall area of Koh Kao Yai Islands

low, medium, high, and very high. The grid cell resolution of the map is 30x30 meters. The high potential area is abundantly covered in the Koh Kao Yai Islands, particularly in the Prasat Hin Pan Yod chamber (Fig. 4). Types of the sinkholes as classified by Waltham et al. (2005) do not conduct by the DMR due to the scarcity of fundamental analysis data. However, an enhanced sinkhole potential map is still useful for limestone failure assessment in the Prasat Hin Pan Yod area.

5.3 Rockfall hazard zonation

To examine the overview rock mass stability and select suitable locations for collecting field data, rockfall hazard zonation of the Prasat Hin Pan Yod chamber had mapped by using the approach of simple multi-criteria in GIS. The five basic factors were integrated to analyze and delineate rockfall hazard areas (Fig. 5). They are consisting of density of lines (Fig. 5A), density of intersection points (Fig. 5B), lineament proximity (Fig. 5C), slope (Fig. 5D), and aspect (Fig. 5E). The rockfall hazard zonation resulted in a grid cell size of 5x5 meters and was categorized into 5 classes including very low, low, moderate, high, and very high. The map shows moderate to high level hazard seems to be happening along sea cliffs and at the entrance of tourist sites as well (Fig. 6)

5.4. Rock Mass Rating (RMR) evaluation

The RMR is a geomechanics classification system for rock mass. A sum of each rating values provide overall comprehensive index of rock mass quality or RMR value (Bieniawski, 1989). The RMR values can be estimated through 9 locations (Fig. 7) distributed along the rim of the chamber, a big broken block of limestone, and the new expected entrance of the tourist site. The RMR values ranged from 53 to 62 (Table 1). The result shows that the RMR of the bedded limestone has lower values than the massive limestone. Thinner bedding is stratigraphically overlying on the Massive limestone, so it is hard to explore the unstable rock when the rock mass locates in the high places of the Prasat Hin Pan Yod area.

5.5 Rock failure analysis using Stereographic projection

The rock failure analysis using stereographic projection found that the wedge failure of rockfall has more potential and happens more frequently than toppling and planar, respectively (Table 2). After field checking, the wedge failure was found that tends to occur a small event of rockfall with a small block pending in the cavity and mainly caused unsafely in the tourist site. For toppling failure, oblique toppling and direct toppling have the same situation as planar failure but will be happened in particular locality. Planar failure is the lowest potential of rockfall, but big events with huge block can be happened in recent time, for example, the rockfall event at the Prasat Hin Pan Yod tourist site on February 20, 2021.

The making of stereographic projection from the discontinuous planes on the outcrop slope was used for modeling rock mass failures or rockfall types that can occur in a planar, wedge, or toppling. The rock mass failures were next used to calculate the SMR adjustment factors. Some stations are selected to show as samples of the stereographic projection analysis which shown below (Figs 8, 9, 10 and 11).

5.6 Slope Mass Rating (SMR) assessments

The SMR was developed by Romana (1985) for evaluating rock slope stability. The SMR assessment in the Prasat Hin Pan Yod area can be divided into 4 sub-areas with totally 26 of SMR stations (Fig. 12).

1) The area of rockslide on February 20, 2021 that nowadays hiding the Prasat Hin Pan Yod entrance, in which was represented by the stations of 1A to1E, 3A to 3D, and 7A to 7F.

2) The strait locating between linearly sea cliff and the former huge topple of rock mass, in which was illustrated by the stations of 4A, and 6A to 6C.

3) A high eroded sea cave with clues of former rockfall and thin column supporting with high potential hazard, which representative stations was composed of 2A to 2C.

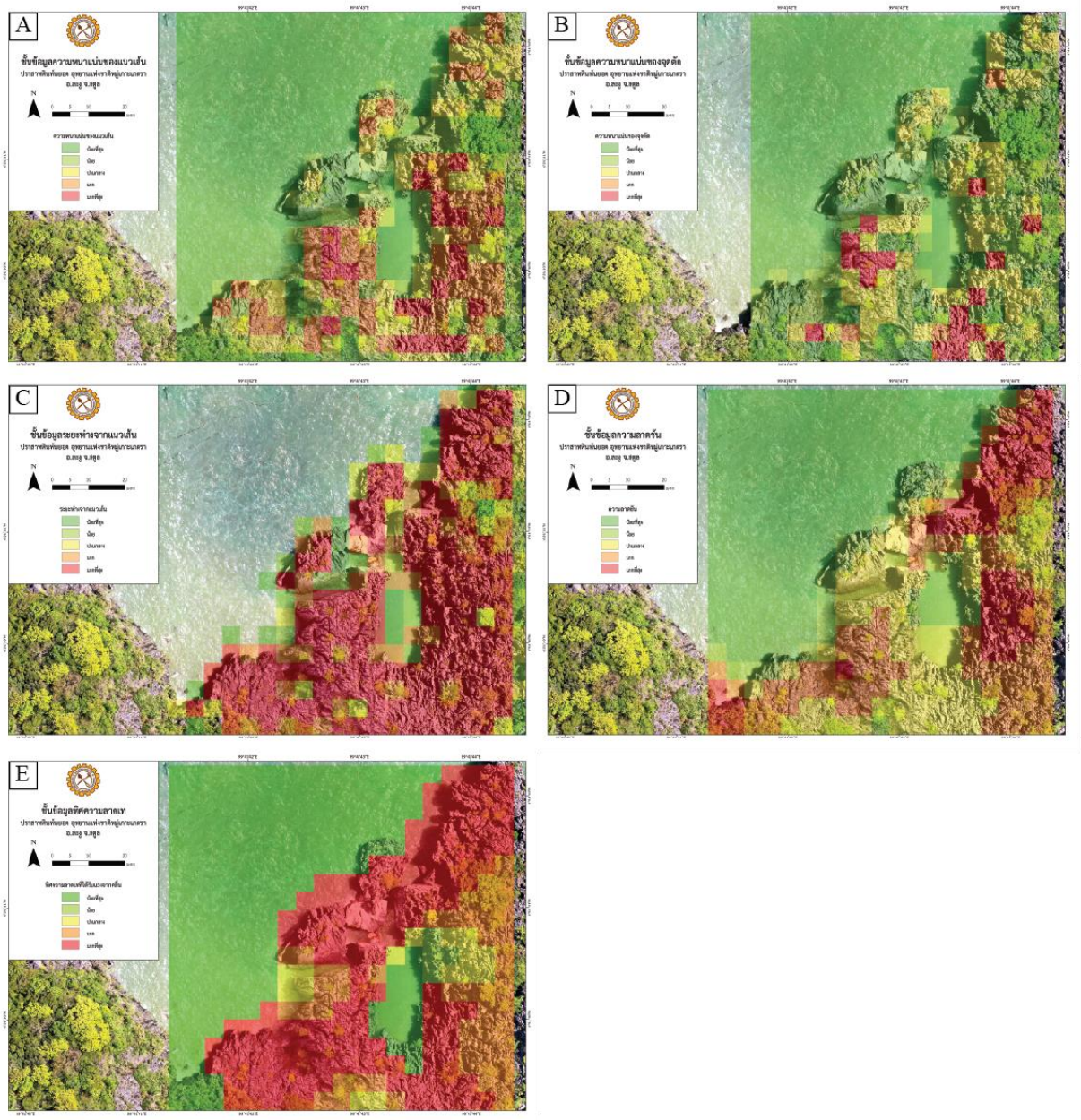

Fig.5 Five factors for preliminary rockfall hazard mapping using GIS; (A) density of lines, (B) density of intersection points, (C) Lineament proximity, (D) slope, and (E) aspect.

Fig. 6 preliminary rockfall hazard map, the Prasat Hin Pan Yod tourist site, Satun province.

Table 1 The summary of RMR value obtained from the field investigation

Station	UCS	RQD	joint spacing	Persistent	Aperture	joint roughness	Filling	Weathering	GW	Discontinuity orientation	RMR
1	54.29	75.38	117.78 cm	4.87 m	20-30 mm	rough	none	moderate	Flowing	none	**55**
	7	17	15	2	0	5	6	3	0	0	
2	54.83	95.68	60,80, 100cm	6.05 m	5-10 mm	rough	none	moderate	Flowing	Dip 0-20 irrespective of strike	**53**
	7	20	15	2	0	5	6	3	0	-5	
3	61.78	75.38	118.78cm	10.69 m	20-30 mm	rough	none	moderate	Flowing	none	**54**
	7	17	15	1	0	5	6	3	0	0	
4	63.39	95.7	65 cm	3 m	20 mm	very rough	none	moderate	Flowing	none	**59**
	7	20	15	2	0	6	6	3	0	0	
5	56.84	92.09	60 cm	3,10 m	5 mm	rough	none	moderate	tidal	none	**59**
	7	20	15	2	1	5	6	3	0	0	
6	61.78	93	110 cm	3 m	12 mm	very rough	none	moderate	Flowing	none	**59**
	7	20	15	2	0	6	6	3	0	0	
7	61.24	75.38	70 cm	10 m	10 mm	rough	none	moderate	Flowing	none	**55**
	7	17	15	2	0	5	6	3	0	0	
8	54.83	91.48	60, 100 cm	3 m	5 mm	very rough	none	moderate	tidal	none	**62**
	7	20	15	4	1	6	6	3	0	0	
9	58.23	96.91	64 cm	12.6m	10 mm	rough	none	moderate	tidal	none	**57**
	7	20	15	1	0	5	6	3	0	0	

Note: UCS = Uniaxial Compressive Strength, RQD = Rock Quality Designation which was proposed by Deere (1964), and GW = Groundwater

Fig. 7 showing stations of measured Rock Mass Rating overlying on orthophoto

Table 2 The summary of rock failure analysis using stereographic projection

Station	No.	Face slope (Dip direction/ Dip angle)	Failure mode					
			Planar (%)	Wedge (%)	Toppling (%)			
					Direct	Oblique	Flexural	Base plane
1	1A	003/85	0	25.15	15.2	9.36	0	0
	1B	355/88	0	42.69	16.96	9.36	0	21.05
	1C	087/88	26.32	59.06	10.53	12.87	0	36.84
	1D	317/89	10.53	50.88	2.92	25.15	0	10.53
	1E	233/78	21.05	35.09	21.64	34.5	10.53	21.05
2	2A	325/80	0	1.11	11.11	47.78	21.43	0
	2B	255/83	14.29	40	5.56	13.33	0	14.29
	2C	225/84	21.43	64.44	10	4.44	0	21.43
	2D	353/85	0	3.33	18.89	50	21.43	7.14
3	3A	020/89	20	46.67	0	0	0	40
	3B	095/89	33.33	32.38	10.48	1.9	6.67	40
	3C	328/87	6.67	35.24	0.95	9.52	0	26.67
	3D	122/87	0	18.1	13.33	3.81	6.67	6.67
4	4A	260/78	12.5	45	12.5	17.5	18.75	18.75
5	5A	062/85	0	0	0	10	0	20
6	6A	004/81	0	1.9	3.33	39.52	4.76	14.29
	6B	163/72	0	0.95	8.1	33.81	28.57	0
	6C	337/81	0	5.24	0	26.67	0	14.29
7	7A	245/78	9.09	22.92	35.04	12.12	12.12	9.09
	7B	264/83	6.06	18.75	17.23	9.28	3.03	6.06
	7C	324/77	9.09	21.97	0.57	4.55	24.24	18.18
	7D	222/77	9.09	17.61	29.92	13.26	18.18	9.09
	7E	290/82	9.09	23.67	4.92	4.92	12.12	12.12
	7F	110/82	12.12	42.8	6.63	10.23	12.12	21.21
8	8A	034/85	0	17.65	5.88	13.07	0	22.22
9	9A	022/85	10	22.22	4.44	22.22	0	30

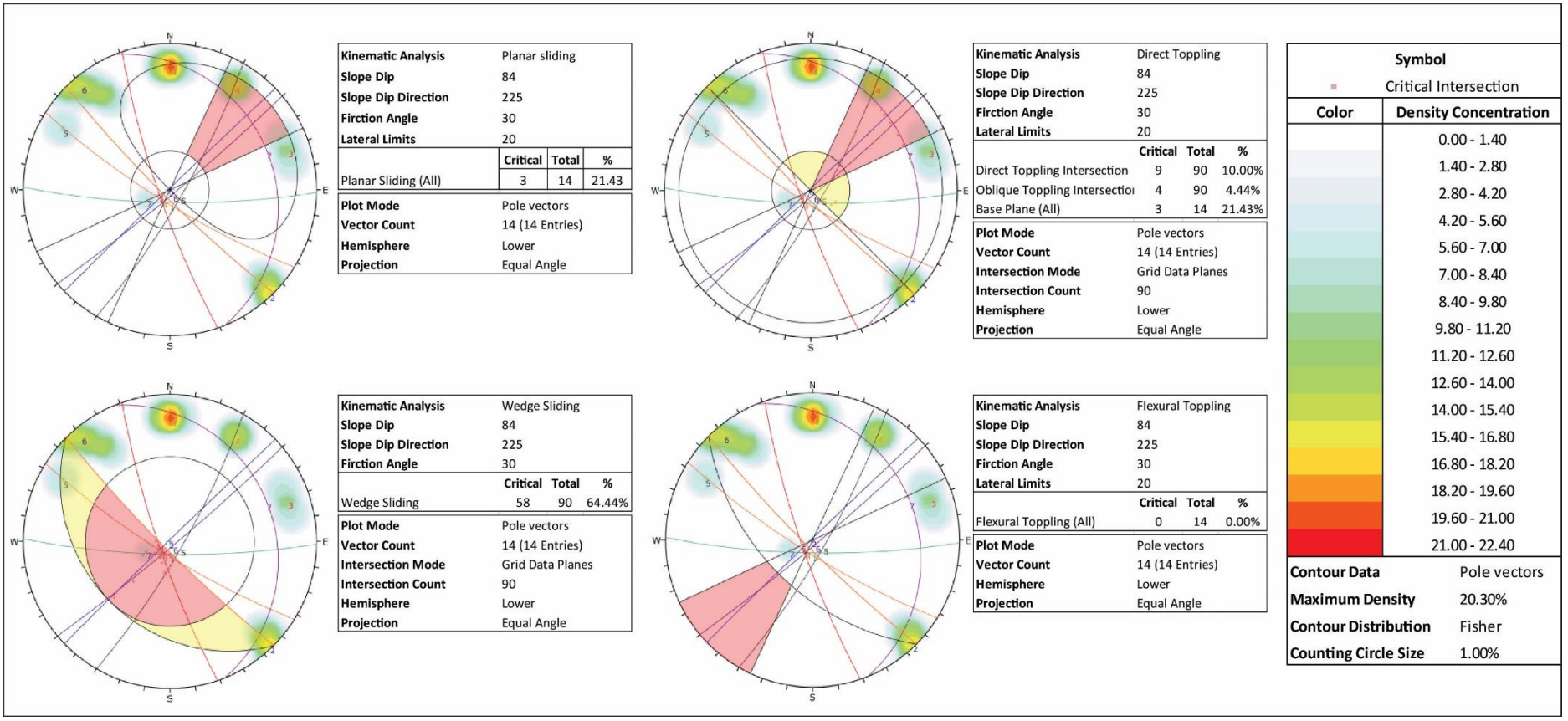

Fig. 8: showing stereographic projection of the station 2C

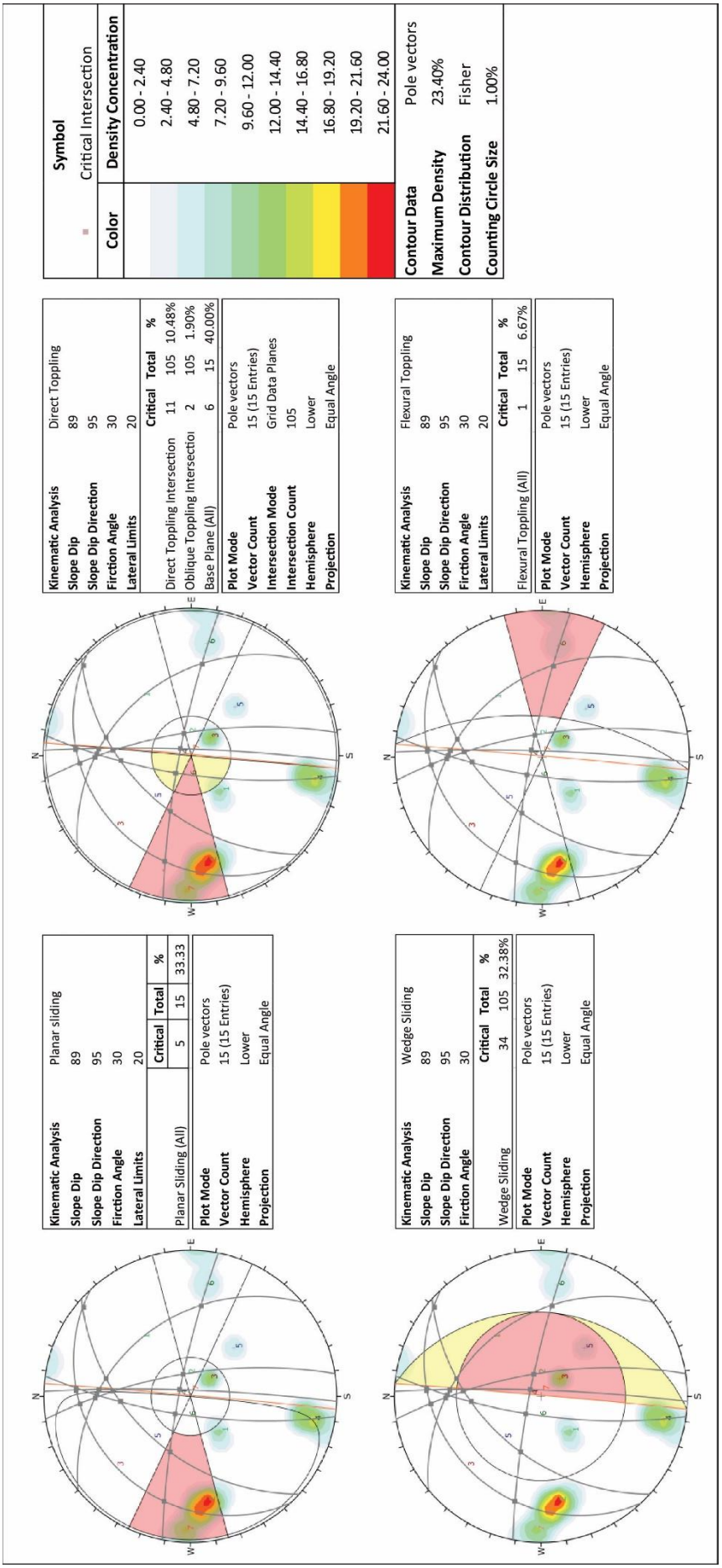

Fig.9: showing stereographic projection of the station 3B

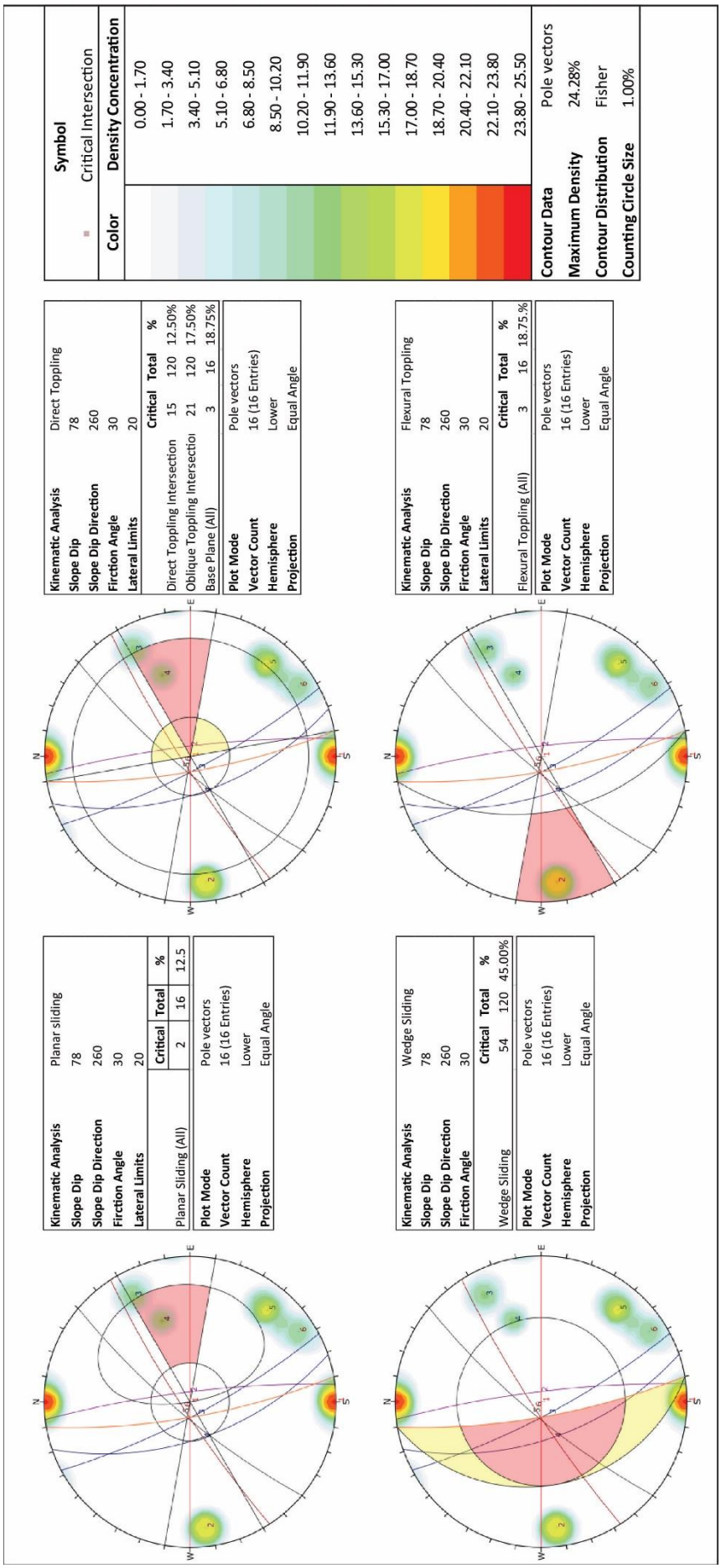

Fig. 10: showing stereographic projection of the station 4A

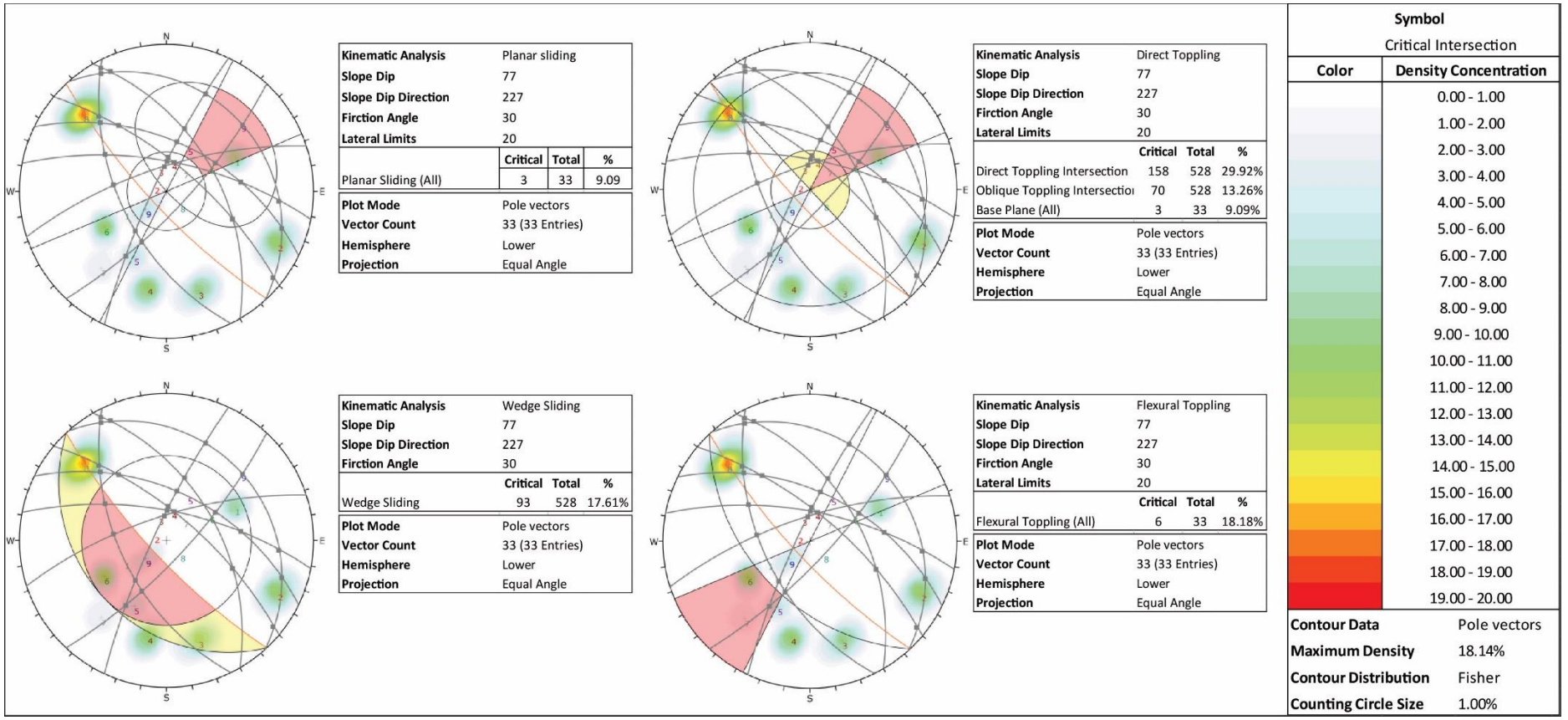

Fig. 11: showing stereographic projection of the station 7D

Fig. 12: showing stations of Slope Mass Rating (SMR) assessment

4) A small beach within the Prasat Hin Pan Yod chamber that exposed whenever low tide, the representative stations were 8A and 9A.

SMR was calculated and classified according to Romana (1985). The SMR assessment in detail of station 2A and station 4A was partly shown in Table 3 and Table 4, respectively. The overall result of the 26 stations was depicted in Table 5 and was shortly summarized in Table 6

Station 1A to 1E is the previous entrance of the Prasat Hin Pan Yod tourist site which is concealed from a huge block of the rockslide. Stations 1A to 1E had an SMR value of 27.5-70.1275, which was classified as bad to good (Table 5). The dominant SMR values were categorized as a good class. There were two intersections of joint sets of wedge failure, and one of the joint planes of toppling failure was classified as a normal class. Additionally, two points intersections of joint sets had an SMR score of 27.5, which was classified as low class. For such the representative SMR, wedge failure of rockfall type has so higher potential to have occurred in stations 1A to 1E. The three intersections (Table 6), plunging to nearly north (NNE) nearly east, and also southwest (SW) may be originated from wedge failure of rockfall type. As mentioned, the tourist route for the inner chamber should not pass stations 1A, 1C, and 1E.

Station 2A (Fig. 13) is a place of the sea cave that locating beneath a massive limestone roof and supported by a thin column. The evidence of a former rockfall had two big blocks. Due to the high energy of currents and waves, rock collapse might have occurred in nearly future. The SMR value's wedge failure (Table 3 and 5) was categorized as bad and very bad. The SMR value was 8-18 and 25.5-33, respectively. Wedge failure of rockfall type has a higher potential to have occurred than planar and toppling failure. Moreover, bedding rockfall blocks is one of the high potential hazards, and it is difficult to determine by the SMR approach.

Station 3A-3D is the lower part of the broken rock that remained from the rockslide event in February 2021. The SMR value was range 18-69 (Table 5), and it was almost categorized as a good class and normal class. The SMR value of direct toppling failure was partly categorized as very bad (two values) to bad (one value), meanwhile, four SMR value

Table 4 Some of the evaluating result of Slope Mass Rating (SMR) at the station 2A

Failure mode	Face slope	joint sets	Trend	Plunge	RMR	F1	F2	F3	F4	F1F2F3 +F4	SMR	Class	Stability
Planar	225/84	120/80	-	-	53	105	80	-4	Natural	7.5	60.5	Normal	Partially stable
						0.15	1	-50	15				
	225/84	318/89	-	-	53	91	89	5	Natural	14.1	67.1	Good	Stable
						0.15	1	-6	15				
	225/84	140/86	-	-	53	85	86	2	Natural	14.1	67.1	Good	Stable
						0.15	1	-6	15				
	225/84	68/19	-	-	53	157	19	-65	Natural	13.65	66.65	Good	Stable
						0.15	0.15	-60	15				
Wedge	225/84	251/88, 316/89	232	80	53	7	80	-4	Natural	-27.5	25.5	Bad	Unstable
						0.85	1	-50	15				
	225/84	251/81, 140/86	210	78	53	15	78	-6	Natural	-20	33	Bad	Unstable
						0.7	1	-50	15				
	225/84	251/81, 212/80	223	80	53	2	80	-4	Natural	-35	18	Very Bad	Completely unstable
						1	1	-50	15				
	225/84	251/81, 120/80	184	68	53	41	68	-16	Natural	6	59	Normal	Partially stable
						0.15	1	-60	15				
	225/84	251/81, 181/80	212	78	53	13	78	-6	Natural	-20	33	Bad	Unstable
						0.7	1	-50	15				
	225/84	316/89, 140/86	227	39	53	2	39	-45	Natural	-45	8	Very Bad	Completely unstable
						1	1	-60	15				
	225/84	316/89, 212/80	231	79	53	6	79	-5	Natural	-27.5	25.5	Bad	Unstable
						0.85	1	-50	15				
	225/84	181/80, 140/86	210	79	53	15	79	-5	Natural	-20	33	Bad	Unstable
						0.7	1	-50	15				
	225/84	181/80, 316/89	230	75	53	5	75	-9	Natural	-27.5	25.5	Bad	Unstable
						0.85	1	-50	15				
Direct Toppling	225/84	181/80	-	-	53	224	1	164	Natural	11.25	64.25	Good	Stable
						0.15	1	-25	15				
	225/84	120/80	-	-	53	285	1	164	Natural	11.25	64.25	Good	Stable
						0.15	1	-25	15				
	225/84	316/89	-	-	53	89	1	173	Natural	11.25	64.25	Good	Stable
						0.15	1	-25	15				
	225/84	140/86	-	-	53	265	1	170	Natural	11.25	64.25	Good	Stable
						0.15	1	-25	15				
Flexural Toppling	225/84	120/80	-	-	53	285	1	164	Natural	11.25	64.25	Good	Stable
						0.15	1	-25	15				
	225/84	316/89	-	-	53	89	1	173	Natural	11.25	64.25	Good	Stable
						0.15	1	-25	15				
	225	140/89	-	-	53	265	1	173	Natural	11.25	64.25	Good	Stable
						0.15	1	-25	15				

of wedge failure was classified as a bad class. The very bad to bad SMR class of direct toppling failure had a joint plan dipping to the east. The bad SMR class of wedge failure hadfive intersects of joint sets plunging to the northwest and nearly north (Table 6) and it maybe caused by wedge failure of rockfall type. Although the SMR value of planar failure is classified as a normal class, the rockslide can be occurred as well particularly, in the case of repeatedly column supporting broken. For safety, the tourist route should not pass station 3A-3D getting through the Prasat Hin Pan Yod chamber.

Station 4A (Fig. 13) had SMR value of 23-74, which is classified as bad to good. The five intersects of joint sets were classified as bad class (Table 4 and Table 5). The intersection of joint sets plunges to the west and southwest which shows potential wedge failure of rockfall hazard type (Table 6). Tourists may be slightly affected by small pieces of rock wedge that pending at high places. Fortunately, distance passing station 4A and getting through is quite short (not over 3 meters).

Station 5A had SMR value of 70.25-74 (Table 5 and 6) and all SMR values were classified as good class. It can be said that limestone rock mass having stable and safety for tourist.

Station 6A to 6C had SMR score of 56.65-73.1 (Table 5 and Table 6) which all SMR values were classified as normal to good class. There was none of bad to very bad. However, rockfall hazard may be originated by both direct and oblique toppling

Table 4 Some of the evaluating result of Slope Mass Rating (SMR) at the station 4A

Failure mode	Face slope	joint sets	Trend	Plunge	RMR	F1	F2	F3	F4	F1F2F3 +F4	SMR	Class	Stability
Planar	260/78	360/90	-	-	59	100	90	12	Natural	15	74	Good	Stable
						0.15	1	0	15				
	260/78	083/82	-	-	59	177	82	4	Natural	14.1	73.1	Good	Stable
						0.15	1	-6	15				
	260/78	327/83	-	-	59	67	83	5	Natural	14.1	73.1	Good	Stable
						0.15	1	-6	15				
Wedge	260/78	310/79, 327/83	262	74	59	2	74	-4	Natural	-35	24	Bad	Unstable
						1	1	-50	15				
	260/78	360/90, 251/61	270	60	59	10	60	-18	Natural	-36	23	Bad	Unstable
						0.85	1	-60	15				
	260/78	251/61, 327/83	250	61	59	10	61	-17	Natural	-36	23	Bad	Unstable
						0.85	1	-60	15				
	260/78	242/79, 310/79	276	77	59	16	77	-1	Natural	-20	39	Bad	Unstable
						0.7	1	-50	15				
	260/78	251/61, 310/79	240	61	59	20	61	-17	Natural	-27	32	Bad	Unstable
						0.7	1	-60	15				
	260/78	242/79, 327/83	271	78	59	11	78	0	Natural	-2.5	56.5	Normal	Partially stable
						0.7	1	-25	15				
	260/78	242/79, 251/61	327	23	59	67	23	-55	Natural	11.4	70.4	Good	Stable
						0.15	0.4	-60	15				
Direct Toppling	260/78	360/90	-	-	59	80	1	168	Natural	11.25	70.25	Good	Stable
						0.15	1	-25	15				
	260/78	083/82	-	-	59	357	1	160	Natural	11.25	70.25	Good	Stable
						0.15	1	-25	15				
	260/78	327/83	-	-	59	357	1	161	Natural	11.25	70.25	Good	Stable
						0.15	1	-25	15				
	260/78	310/79	-	-	59	130	1	157	Natural	11.25	70.25	Good	Stable
						0.15	1	-25	15				
Flexural Toppling	260/78	360/90	-	-	59	80	1	168	Natural	11.25	70.25	Good	Stable
						0.15	1	-25	15				
	260/78	327/83	-	-	59	113	1	161	Natural	11.25	70.25	Good	Stable
						0.15	1	-25	15				
	260/78	251/61	-	-	59	189	1	139	Natural	11.25	70.25	Good	Stable
						0.15	1	-25	15				
	260/78	310/79	-	-	59	130	1	157	Natural	11.25	70.25	Good	Stable
						0.15	1	-25	15				

Station 7A to 7F is the huge block of planar rockslide that occurred by column supporting broken in the event of February 2021. The investigated stations had SMR values of 19-70 (Table 5 and Table 6), which were classified as very bad to good. The dominant SMR values were categorized as a good class. Two intersections of joint sets of wedge failure had SMR value of 19, which were categorized as a very bad class. There were five intersections of joint sets of wedge failure, which were classified as a bad class (28-34.3).

Furthermore, four intersections of joint sets of wedge failure and one joint plan of direct toppling were classified as a normal class, which still had partially stable. The rock movement direction was mainly plunging west to northwest (W-NW) and southeast to southwest (SE-SW) (Table 6). As mentioned, tourists should not close up the huge block of planar rockslide located nearby sea cliff because of rockfall, particularly small wedge shape hanging on the high place.

Station 8A had SMR score of 35-7.77 (Table 5) which the dominant values were classified as good class (Table 6). There was only one intersects of joint sets that classified as bad class. Rockfall hazard may be caused by wedge failure. Because of intersection of joint sets plunging to northeast (NE), tourist should be aware pieces of rock wedge that pending at high place in the Prasat Hin Pan Yod chamber.

Station 9A had SMR score of 29.5-69.6 (Table 5). The SMR value was mostly classified as good class. There was only one joint plan dipping to nearly north (NNE) (Table 6), planar failure may be originated rockfall in the Prasat Hin Pan Yod chamber.

Fig. 13: photograph of station 2A (right) and station 4A (left)

5.7 Support guidelines for stabilization

Most SMR values are classified the rock slope as a good class. Some SMR values have lower than 10 due to error of under estimation or rock failure occurred already. None of slope having an SMR value below 10 exist in nature. SMR value below 20 may cause the rock slope failure very quickly. Detailed studies should be carried out where an SMR value is less than 40 (or IVa to Va) because tourist sites are in danger and the rock slope should be stabilized by the integration of various measures: bolting/anchors, shotcrete, diversion drains and removal of rock fragment at high place as following in Table 7. In National Park and Satun Geopark, a safe slope angle should be determined to increase SMR to 60.

6. Conclusions

Preliminary rockfall zonation mapping is useful for field investigation. For the better quality of mapping, field data and more parameters relate to rockfall occurrence have to be added to GIS analysis. Paleo-collapse sinkhole at coastal zone can be recurrent at the place having weakened or cavernous rockmass and high force of the sea process. The new collapse often happens at the rime of sinkhole chamber by various failure mechanisms: planar, wedge, and topple, and the event show as rockslide and rockfall.

The rockfall is defined as the one of the major geohazards in the Prasat Hin Pan Yod area. It is mainly caused by the wedge failure mechanism. Topple and planar failure is subordinate to rockfall and rockslide hazards.

The former route getting through the chamber (stations of 1A to1E, 3A to 3D, and 7A to 7F) should be avoided due to having high potential rockfall of wedge failure. Toppling and planar failure have a lower potential to be originated rockfall hazards. The rockfall hazard is expected to have occurred in small events, but it is high frequency.

The line of stations 4A and 6A to 6C are said to be the safest new route to getting through the chamber. However, the wedge failure of rockfall can occur within a short distance of a sea cliff (about 3 meters). A helmet, one of the simple tools, can protect tourists from fallen rock which it is pending on sea cliffs or high places. For the linear strait, the route is narrow, and slightly strong waves in some time, kayak carrying tourists passing should be controlled and permit a one for in and out.

A limitation of the tourist number is essential for the Prasat Hin Pan Yod chamber. Tourists can spend their time in the chamber, but they must be aware of the rockfalls of wedge failures, and avoid visitation near sea caves that it locates beneath massive limestone.

Because the Prasat Hin Pan Yod has located nearby a strait, the strong wave and currents in the monsoon period can cause the broken block to be moved, titling, or morefracturing. Rock mass stability and slope mass stability still need long-term site investigation and monitoring at the sea cliffs and the rim of the sinkhole chamber; therefore, Real-time kinematic (RTK) surveying will use for detecting rock displacement

Table 5 The result of SMR assessment in the Prasat Hin Pan Yod tourist site

Station	No.	RMR	Flace slope	Failure analysis of Stereonet analysis			SMR				A number of SMR class in failure mode				
				Failure modes	%	Number of joint or intersection	Range		Mode		Very Bad	Bad	Normal	Good	Very good
							min	max	SMR value	SMR class	0-20	21-40	41-60	61-80	81-100
1	1A		003/85	Planar	0	0									
				Wedge	25.15	5	27.5	69.1	none	Good	0	1	0	4	0
				Direct Toppling	15.2	8	52.5	66.25	66.25	Good	0	0	1	7	0
				Oblique Toppling	9.36										
				Flexural Toppling	0	0									
	1B		355/88	Planar	0	0									
				Wedge	42.69	7	52.5	68.65	62.5	Good	0	0	1	6	0
				Direct Toppling	16.96	5	66.25	66.25	66.25	Good	0	0	0	5	0
				Oblique Toppling	9.36										
				Flexural Toppling	0	0									
	1C		087/88	Planar	26.32	2	61	66.25	none	Good	0	0	0	2	0
				Wedge	59.06	3	27.5	66.25	none	Good	0	1	0	2	0
				Direct Toppling	10.53	4	66.25	66.25	66.25	Good	0	0		4	0
				Oblique Toppling	12.87										
				Flexural Toppling	0	0									
	1D		317/89	Planar	10.53	2	61	62.5	none	Good	0	0	0	2	0
				Wedge	50.88	5	50	62.5	61	Good	0	0	1	4	0
				Direct Toppling	2.92	5	66.25	66.25	66.25	Good	0	0	0	5	0
				Oblique Toppling	25.15										
				Flexural Toppling	0	0									
	1E	55	233/78	Planar	21.05	1	70.1275	70.1275	70.1275	Good	0	0	0	1	0
				Wedge	35.09	3	27.5	61	61	Good	0	1	0	2	0
				Direct Toppling	21.64	8	66.25	66.25	66.25	Good	0	0	0	8	0
				Oblique Toppling	34.5	1	66.25	66.25	66.25	Good	0	0	0	1	0
				Flexural Toppling	10.53										
2-JO	2A	53	325/80	Planar	0	0									
				Wedge	1.11	2	59	64.25	59, 64.25	Normal, Good	0	0	1	1	0
				Direct Toppling	11.11	13	64.25	64.25	64.25	Good	0	0	0	13	0
				Flexural Toppling	21.43	1	64.25	65.25	66.25	Good	0	0	0	1	0
				Oblique Toppling	47.78										
	2B		255/83	Planar	14.29	3	60.5	67.1	none	Good	0	0	1	0	2
				Wedge	40	9	48	60.5	60.5	Normal	0	0	9	0	0
				Direct Toppling	5.56	6	64.25	64.25	64.25	Good	0	0	0	6	0
				Oblique Toppling	13.33										
				Flexural Toppling	0	0									
	2C		225/84	Planar	21.43	4	60.5	67.1	67.1	Good	0	0	1	3	0
				Wedge	64.44	9	8	59	25.5	Bad	2	6	1	0	0
				Direct Toppling	10	4	64.25	64.25	64.25	Good	0	0	0	4	0
				Oblique Toppling	4.44										
				Flexural Toppling	0	0									
	2D		353/85	Planar	0	2	60.5	60.5	60.5	Normal	0	0	2	0	0
				Wedge	3.33	4	59	66.65	59, 66.65	Normal, Good	0	0	2	2	0
				Direct Toppling	18.89	6	64.25	64.25	64.25	Good	0	0	0	6	0
				Oblique Toppling	50	2	64.25	65.25	66.25	Good	0	0	0	2	0
				Flexural Toppling	21.43										
3	3A	54	020/89	Planar	20	3	60	61.5	60	Good	0	0	2	1	0
				Wedge	46.67	15	34	67.65	52.5	Normal	0	3	7	5	0
				Direct Toppling	0	4	65.25	65.25	65.25	Good	0	0	0	4	0
				Flexural Toppling	0	0									
				Oblique Toppling	0	0									
	3B		095/89	Planar	33.33	4	60	65.4	60	Normal	0	0	2	2	0
				Wedge	32.38	14	45	67.65	65.4, 67.65	Good	0	0	3	11	0
				Direct Toppling	10.48	9	9	60	60	Normal	2	1	6	0	0
				Flexural Toppling	6.67	6	60	60	60	Normal	0	0	6	0	0
				Oblique Toppling	1.9										
	3C		328/87	Planar	6.67	1	61.35	61.35	61.35	Good	0	0	0	1	0
				Wedge	35.24	9	27	65.4	65.4	Good	0	1	2	6	0
				Direct Toppling	0.95	5	65.25	66.25	67.25	Good	0	0	0	5	0
				Oblique Toppling	9.52										
				Flexural Toppling	0	0									
	3D		122/87	Planar	0	0									
				Wedge	18.1	4	59.4	67,65	none	Normal, Good	0	0	2	2	0
				Direct Toppling	13.33	11	47.75	69	65.25	Good	0	0	4	7	0
				Oblique Toppling	3.81										
				Flexural Toppling	6.67	4	65.25	68.1	65.25	Good	0	0	0	4	0
4	4A	59	260/78	Planar	12.5	3	73.1	74	73.1	Good	0	0	0	3	0
				Wedge	45	7	23	70.4	23	Bad	0	5	1	1	0
				Direct Toppling	12.5	4	70.25	71.25	72.25	Good	0	0	0	4	0
				Oblique Toppling	17.5										
				Flexural Toppling	18.75	4	70.25	70.25	70.25	Good	0	0	0	4	0
5	5A	59	062/85	Planar	0	0									
				Wedge	0	0									
				Direct Toppling	0	0									
				Oblique Toppling	10	3	70.25	74	70.25	Good	0	0	0	3	0
				Flexural Toppling	0	0									
6	6A	59	004/81	Planar	0	0									
				Wedge	1.9	11	66.5	73.1	73.1	Good	0	0	0	11	0
				Direct Toppling	3.33	15	52.75	70.25	70.25	Good	0	0	2	0	0
				Oblique Toppling	39.52										
				Flexural Toppling	4.86	3	70.25	74	70.25	Good	0	0	0	3	0
	6B		163/72	Planar	0	0									
				Wedge	0.95	4	73.1	74	74	Good	0		0	4	0
				Direct Toppling	8.1	16	52.75	70.25	70.25	Good	0	0	4	12	0
				Oblique Toppling	33.81										
				Flexural Toppling	28.57	2	70.25	70.25	70.25	Good	0		0	2	0
	6C		337/81	Planar	0	0									
				Wedge	5.24	5	65	73.1	66.5	Good	0	0	0	5	0
				Direct Toppling	0	0									
				Oblique Toppling	26.67	15	70.25	70.25	70.25	Good	0	0	0	15	0
				Flexural Toppling	0	0									
7-JO	7A	55	245/78	Planar	9.09	6	61	66.4	61	Good	0	0	0	6	0
				Wedge	22.92	11	46	68.5	68.5	Good	0	0	1	10	
				Direct Toppling	35.04	7	66.25	70	66.25	Good	0	0	0	7	0
				Oblique Toppling	12.12										
				Flexural Toppling	12.12	4	66.25	66.25	66.25	Good	0	0	0	4	0
	7B		264/78	Planar	6.06	6	61	66.4	61	Good	0	0	0	6	0
				Wedge	18.75	8	28	66.4	61,62.35,66.	Good	0	1	0	7	0
				Direct Toppling	17.23	8	66.25	70	66.25	Good	0	0	0	8	0
				Oblique Toppling	9.28										
				Flexural Toppling	3.03	3	66.25	66.25	66.25	Good	0	0	0	3	0
	7C		324/77	Planar	9.09	3	61	62.5	61	Good	0	0	0	3	0
				Wedge	21.97	12	28	68.65	62.5	Good	0	1	2	9	0
				Direct Toppling	0.57	6	66.25	67.25	68.25	Good	0	0	0	6	0
				Oblique Toppling	4.55										
				Flexural Toppling	24.24	10	66.25	70	66.25	Good	0	0	0	10	0
	7D		227/77	Planar	9.09	7	61	69.1	62.5	Good	0	0	0	7	0
				Wedge	17.61	5	19	62.35	none	Good	1	1	1	2	0
				Direct Toppling	29.92	8	61	61	61	Good	0	0	0	8	0
				Oblique Toppling	13.26										
				Flexural Toppling	18.18	5	61	61	61	Good	0	0	0	5	0
	7E		290/82	Planar	9.09	5	61	66.4	61	Good	0	0	0	5	0
				Wedge	23.67	12	28	62.35	61	Good	0	2	0	10	0
				Direct Toppling	4.92	9	66.25	70	66.25	Good	0	0	0	9	0
				Oblique Toppling	4.92										
				Flexural Toppling	12.12	6	66.25	66.25	66.25	Good	0	0	0	6	0
	7F		110/82	Planar	12.12	4	61	61	61	Good	0	0	0	4	0
				Wedge	42.8	12	19	68.65	61	Good	1	0	1	10	0
				Direct Toppling	6.63	8	48.75	66.25	67.25	Good	0		2	6	0
				Oblique Toppling	10.23										
				Flexural Toppling	12.12	10	66.25	70	66.25	Good	0	0	0	10	0
8	8A	62	034/85	Planar	0	0									
				Wedge	17.65	5	35	75.65	none	Good	0	1	0	4	0
				Direct Toppling	5.88	4	73.25	77	73.25	Good	0	0	0	4	0
				Oblique Toppling	13.07										
				Flexural Toppling	0	0									
9	9A	57	022/85	Planar	10	3	29.5	69.6	none	Good	0	1	0	2	0
				Wedge	12.12	3	63	68.4	63	Good	0	0	0	3	0
				Direct Toppling	4.44	3	68.25	68.25	69.25	Good	0	0	0	3	0
				Oblique Toppling	22.22										
				Flexural Toppling	0	0									

Table 6 The summary of SMR, failure mode, critical joints, and intersections

Station	No.	Face slope	Failures	Intersection point	joint sets	RMR	SMR	SMR class	SMR stability
1	1A	003/85	Wedge	031/85	086/87,323/88	55	60	Normal	Partially stable
			Wedge	010/80	086/87,045/80	55	27.5	Bad	Unstable
			Direct Toppling	none	171/59	55	52.5	Normal	Partially stable
	1B	355/88	Wedge	341/88	360/88,323/88	55	52.5	Normal	Partially stable
	1C	087/88	Wedge	081/78	360/88,045/80	55	27.5	Bad	Unstable
	1D	317/89	Wedge	341/88	360/88,323/88	55	50	Normal	Partially stable
	1E	233/78	Wedge	238/69	224/70,323/88	55	27.5	Bad	Unstable
2	2A	325/80	Wedge	045/55	316/89,120/80	53	59	Normal	Partially stable
	2B	255/83	Wedge	232/80	251/88,316/89	53	48	Normal	Partially stable
			Wedge	227/39	316/89,140/86	53	47.6	Normal	Partially stable
			Wedge	231/79	316/89,212/80	53	48	Normal	Partially stable
			Wedge	230/75	181/80,316/89	53	49	Normal	Partially stable
	2C	225/84	Wedge	232/80	251/88,316/89	53	25.5	Bad	Unstable
			Wedge	210/78	251/81,140/86	53	33	Bad	Unstable
			Wedge	223/80	251/81,212/80	53	18	Very Bad	Completely unstable
			Wedge	212/78	251/81,181/80	53	33	Bad	Unstable
			Wedge	227/39	316/89,140/86	53	8	Very Bad	Completely unstable
			Wedge	231/79	316/89,212/80	53	25.5	Bad	Unstable
			Wedge	210/79	181/80,140/86	53	33	Bad	Unstable
			Wedge	230/75	181/80,316/89	53	25.5	Bad	Unstable
	2D	353/85	Wedge	045/55	120/80,316/89	53	59	Normal	Partially stable
			Wedge	062/72	120/80,140/86	53	59	Normal	Partially stable
3	3A	020/89	Planar	none	278/75	54	60	Normal	Partially stable
			Planar	none	312/48	54	60	Normal	Partially stable
			Wedge	311/72	011/81,278/75	54	60	Normal	Partially stable
			Wedge	072/72	011/81,081/72	54	60	Normal	Partially stable
			Wedge	290/46	011/81, 312/48	54	60	Normal	Partially stable
			Wedge	033/80	011/81,092/85	54	34	Bad	Unstable
			Wedge	012/29	312/48,050/35	54	52.2	Normal	Partially stable
			Wedge	004/34	312/48,081/72	54	39.6	Bad	Unstable
			Wedge	005/34	312/48, 092/85	54	39.6	Bad	Unstable
			Wedge	004/26	050/35, 092/85	54	52.2	Normal	Partially stable
			Wedge	001/25	050/35,278/75	54	52.2	Normal	Partially stable
			Wedge	000/26	081/72, 278/75	54	52.2	Normal	Partially stable
	3B	095/89	Planar	none	312/48	54	60	Normal	Partially stable
			Planar	none	278/75	54	60	Normal	Partially stable
			Wedge	097/26	011/81,050/35	54	45	Normal	Partially stable
			Wedge	072/72	011/81,081/72	54	60	Normal	Partially stable
			Wedge	311/72	011/81278/75	54	60	Normal	Partially stable
			Direct Toppling	none	312/48	54	60	Normal	Partially stable
			Direct Toppling	none	317/20	54	60	Normal	Partially stable
			Direct Toppling	none	011/81	54	60	Normal	Partially stable
			Direct Toppling	none	278/75	54	9	Very Bad	Completely unstable
			Direct Toppling	none	092/85	54	60	Normal	Partially stable
			Flexural Toppling	none	050/35	54	60	Normal	Partially stable
			Flexural Toppling	none	011/81	54	60	Normal	Partially stable
			Flexural Toppling	none	081/72	54	60	Normal	Partially stable
	3C	328/87	Wedge	290/46	011/81,312/48	54	60	Normal	Partially stable
			Wedge	311/72	011/81,278/75	54	27	Bad	Unstable
			Wedge	072/72	081/72,011/81	54	60	Normal	Partially stable
	3D	122/87	Wedge	072/72	081/72,011/81	54	60	Normal	Partially stable
			Wedge	097/26	050/35,011/81	54	59.4	Normal	Partially stable
			Direct Toppling	none	312/48	54	47.75	Normal	Partially stable
			Direct Toppling	none	278/75	54	59	Normal	Partially stable
4	4A	260/78	Wedge	262/74	310/79,327/83	59	24	Bad	Unstable
			Wedge	270/60	360/90,251/61	59	23	Bad	Unstable
			Wedge	250/61	251/61,327/83	59	23	Bad	Unstable
			Wedge	276/77	242/79,310/79	59	39	Bad	Unstable
			Wedge	240/61	251/61,310/79	59	32	Bad	Unstable
			Wedge	271/78	242/79,327/83	59	56.5	Normal	Partially stable
5	5A	062/65	Oblique Toppling	none	Almost	59	70.25 to 74	Good	Stable
6	6A	004/81	Wedge	none	Almost	59	66.5 to 73.1	Good	Stable
			Direct Toppling	none	Almost	59	64 to 70.25	Good	Stable
			Direct Toppling	none	193/76	59	52.75	Normal	Partially stable
			Direct Toppling	none	196/80	59	56.5	Normal	Partially stable
			Flexural Toppling	none	Almost	59	70.25 to 74	Good	Stable
	6B	163/72	Planar	none	Almost	59	71.6 to 74	Good	Stable
			Direct Toppling	none	Almost	59	70.25	Good	Stable
			Direct Toppling	none	335/86	59	52.75	Normal	Partially stable
			Direct Toppling	none	327/88	59	56.5	Normal	Partially stable
			Direct Toppling	none	356/86	59	56.5	Normal	Partially stable
			Flexural Toppling	none	Almost	59	70.25	Good	Stable
	6C	337/81	Wedge	none	Almost	59	65.5 to 73.1	Good	Stable
			Direct Toppling	none	Almost	59	70.25	Good	Stable
7	7A	245/78	Wedge	218/52	244/55,295/80	55	46	Normal	Partially stable
	7B	264/78	Wedge	277/50	244/55,342/71	55	28	Bad	Unstable
	7C	324/77	Wedge	324/32	026/53,040/69	55	28	Bad	Unstable
			Wedge	316/24	244/55,026/53	55	49.6	Normal	Partially stable
			Wedge	301/38	244/55,011/67	55	49.6	Normal	Partially stable
	7D	227/77	Wedge	218/52	244/55,295/80	55	19	Very Bad	Unstable
			Wedge	206/48	244/55,133/75	55	46	Normal	Partially stable
			Wedge	212/35	295/80,133/75	55	34.3	Bad	Unstable
	7E	290/82	Wedge	277/50	244/55,342/71	55	28	Bad	Unstable
			Wedge	301/38	244/55,011/67	55	34.3	Bad	Unstable
	7F	110/82	Wedge	083/36	011/67,026/53	55	49.6	Normal	Partially stable
			Wedge	113/38	060/52,040/69	55	19	Very Bad	Unstable
			Direct Toppling	none	295/80	55	48.75	Normal	Partially stable
			Direct Toppling	none	277/50	55	52.5	Normal	Partially stable
8	8A	034/85	Wedge	053/51	345/73,128/78	62	35	Bad	Unstable
			Wedge	none	Almost	62	68 to 75.65	Good	Stable
			Direct Toppling	none	Almost	62	73.25 to 77	Good	Stable
9	9A	022/85	Planar	none	014/81	57	29.5	Bad	Unstable
			Wedge	none	Almost	57	63 to 68.4	Good	Stable
			Direct Toppling	none	Almost	57	68.25	Good	Stable

Table 7 Support measures for stabilization based on Singh and Goel (2011)

Station	No.	Face slope	Failures	Intersection point	joint sets	RMR	SMR	SMR class	SMR stability	Suggested Supports
1	1A	003/85	Wedge	031/85	086/87,323/88	55	60	Normal	Partially stable	IIIa
			Wedge	010/80	086/87,045/80	55	27.5	Bad	Unstable	IVb
			Direct Toppling	none	171/59	55	52.5	Normal	Partially stable	IIIa
	1B	355/88	Wedge	341/88	360/88,323/88	55	52.5	Normal	Partially stable	IIIa
	1C	087/88	Wedge	081/78	360/88,045/80	55	27.5	Bad	Unstable	IVb
	1D	317/89	Wedge	341/88	360/88,323/88	55	50	Normal	Partially stable	IIIb
	1E	233/78	Wedge	238/69	224/70,323/88	55	27.5	Bad	Unstable	IVb
2	2A	325/80	Wedge	045/55	316/89,120/80	53	59	Normal	Partially stable	IIIa
	2B	255/83	Wedge	232/80	251/88,316/89	53	48	Normal	Partially stable	IIIb
			Wedge	227/39	316/89,140/86	53	47.6	Normal	Partially stable	IIIb
			Wedge	231/79	316/89,212/80	53	48	Normal	Partially stable	IIIb
			Wedge	230/75	181/80,316/89	53	49	Normal	Partially stable	IIIb
	2C	225/84	Wedge	232/80	251/88,316/89	53	25.5	Bad	Unstable	IVb
			Wedge	210/78	251/81,140/86	53	33	Bad	Unstable	IVa
			Wedge	223/80	251/81,212/80	53	18	Very Bad	Completely unstable	Va
			Wedge	212/78	251/81,181/80	53	33	Bad	Unstable	IVa
			Wedge	227/39	316/89,140/86	53	8	Very Bad	Completely unstable	Error/failure
			Wedge	231/79	316/89,212/80	53	25.5	Bad	Unstable	IVb
			Wedge	210/79	181/80,140/86	53	33	Bad	Unstable	IVa
			Wedge	230/75	181/80,316/89	53	25.5	Bad	Unstable	IVb
	2D	353/85	Wedge	045/55	120/80,316/89	53	59	Normal	Partially stable	IIIa
			Wedge	062/72	120/80,140/86	53	59	Normal	Partially stable	IIIa
3	3A	020/89	Planar	none	278/75	54	60	Normal	Partially stable	IIIa
			Planar	none	312/48	54	60	Normal	Partially stable	IIIa
			Wedge	311/72	011/81,278/75	54	60	Normal	Partially stable	IIIa
			Wedge	072/72	011/81,081/72	54	60	Normal	Partially stable	IIIa
			Wedge	290/46	011/81, 312/48	54	60	Normal	Partially stable	IIIa
			Wedge	033/80	011/81,092/85	54	34	Bad	Unstable	IVa
			Wedge	012/29	312/48,050/35	54	52.2	Normal	Partially stable	IIIa
			Wedge	004/34	312/48,081/72	54	39.6	Bad	Unstable	IVa
			Wedge	005/34	312/48, 092/85	54	39.6	Bad	Unstable	IVa
			Wedge	004/26	050/35, 092/85	54	52.2	Normal	Partially stable	IIIa
			Wedge	001/25	050/35,278/75	54	52.2	Normal	Partially stable	IIIa
			Wedge	000/26	081/72, 278/75	54	52.2	Normal	Partially stable	IIIa
	3B	095/89	Planar	none	312/48	54	60	Normal	Partially stable	IIIa
			Planar	none	278/75	54	60	Normal	Partially stable	IIIa
			Wedge	097/26	011/81,050/35	54	45	Normal	Partially stable	IIIb
			Wedge	072/72	011/81,081/72	54	60	Normal	Partially stable	IIIa
			Wedge	311/72	011/81278/75	54	60	Normal	Partially stable	IIIa
			Direct Toppling	none	312/48	54	60	Normal	Partially stable	IIIa
			Direct Toppling	none	317/20	54	60	Normal	Partially stable	IIIa
			Direct Toppling	none	011/81	54	60	Normal	Partially stable	IIIa
			Direct Toppling	none	278/75	54	9	Very Bad	Completely unstable	Error/failure
			Direct Toppling	none	092/85	54	60	Normal	Partially stable	IIIa
			Flexural Toppling	none	050/35	54	60	Normal	Partially stable	IIIa
			Flexural Toppling	none	011/81	54	60	Normal	Partially stable	IIIa
			Flexural Toppling	none	081/72	54	60	Normal	Partially stable	IIIa
	3C	328/87	Wedge	290/46	011/81,312/48	54	60	Normal	Partially stable	IIIa
			Wedge	311/72	011/81,278/75	54	27	Bad	Unstable	IVb
			Wedge	072/72	081/72,011/81	54	60	Normal	Partially stable	IIIa
	3D	122/87	Wedge	072/72	081/72,011/81	54	60	Normal	Partially stable	IIIa
			Wedge	097/26	050/35,011/81	54	59.4	Normal	Partially stable	IIIa
			Direct Toppling	none	312/48	54	47.75	Normal	Partially stable	IIIb
			Direct Toppling	none	278/75	54	59	Normal	Partially stable	IIIa
4	4A	260/78	Wedge	262/74	310/79,327/83	59	24	Bad	Unstable	IVb
			Wedge	270/60	360/90,251/61	59	23	Bad	Unstable	IVb
			Wedge	250/61	251/61,327/83	59	23	Bad	Unstable	IVb
			Wedge	276/77	242/79,310/79	59	39	Bad	Unstable	IVa
			Wedge	240/61	251/61,310/79	59	32	Bad	Unstable	IVa
			Wedge	271/78	242/79,327/83	59	56.5	Normal	Partially stable	IIIa
5	5A	062/65	Oblique Toppling	none	Almost	59	70.25 to 74	Good	Stable	IIa
6	6A	004/81	Wedge	none	Almost	59	66.5 to 73.1	Good	Stable	IIb to IIa
			Direct Toppling	none	Almost	59	64 to 70.25	Good	Stable	IIb
			Direct Toppling	none	193/76	59	52.75	Normal	Partially stable	IIIa
			Direct Toppling	none	196/80	59	56.5	Normal	Partially stable	IIIa
			Flexural Toppling	none	Almost	59	70.25 to 74	Good	Stable	IIa
	6B	163/72	Planar	none	Almost	59	71.6 to 74	Good	Stable	IIa
			Direct Toppling	none	Almost	59	70.25	Good	Stable	IIb
			Direct Toppling	none	335/86	59	52.75	Normal	Partially stable	IIIa
			Direct Toppling	none	327/88	59	56.5	Normal	Partially stable	IIIa
			Direct Toppling	none	356/86	59	56.5	Normal	Partially stable	IIIa
			Flexural Toppling	none	Almost	59	70.25	Good	Stable	IIb
	6C	337/81	Wedge	none	Almost	59	65.5 to 73.1	Good	Stable	IIb to IIa
			Direct Toppling	none	Almost	59	70.25	Good	Stable	Iib
7	7A	245/78	Wedge	218/52	244/55,295/80	55	46	Normal	Partially stable	IIIb
	7B	264/78	Wedge	277/50	244/55,342/71	55	28	Bad	Unstable	IVb
	7C	324/77	Wedge	324/32	026/53,040/69	55	28	Bad	Unstable	IVb
			Wedge	316/24	244/55,026/53	55	49.6	Normal	Partially stable	IIIb
			Wedge	301/38	244/55,011/67	55	49.6	Normal	Partially stable	IIIb
	7D	227/77	Wedge	218/52	244/55,295/80	55	19	Very Bad	Unstable	Va
			Wedge	206/48	244/55,133/75	55	46	Normal	Partially stable	IIIb
			Wedge	212/35	295/80,133/75	55	34.3	Bad	Unstable	IVa
	7E	290/82	Wedge	277/50	244/55,342/71	55	28	Bad	Unstable	IVb
			Wedge	301/38	244/55,011/67	55	34.3	Bad	Unstable	IVa
	7F	110/82	Wedge	083/36	011/67,026/53	55	49.6	Normal	Partially stable	IIIb
			Wedge	113/38	060/52,040/69	55	19	Very Bad	Unstable	Va
			Direct Toppling	none	295/80	55	48.75	Normal	Partially stable	IIIb
			Direct Toppling	none	277/50	55	52.5	Normal	Partially stable	IIIa
8	8A	034/85	Wedge	053/51	345/73,128/78	62	35	Bad	Unstable	IVa
			Direct Toppling	none	Almost	62	73.25 to 77	Good	Stable	IIa
9	9A	022/85	Planar	none	014/81	57	29.5	Bad	Unstable	IVb
			Wedge	none	Almost	57	63 to 68.4	Good	Stable	IIb
			Direct Toppling	none	Almost	57	68.25	Good	Stable	IIb

References

Bieniawski, Z.T., 1989, Engineering rock mass classification: a complete manual for engineers and geologists in mining, civil, and petroleum engineering (p.250), Wiley and Sons.

Deere, D.U. & Miller, R.P. (1966). Engineering classification and index properties for intact rock. Technical report No. AFNL-TR-65-116 Air Force Weapons Laboratory, New Mexico.

DMR, (2005). Sinkhole potential map of Thailand. Environmental Geology Division, Department of Mineral Resources, Bangkok.

DMR, (2016). Seismic hazard map of Thailand. Environmental Geology Division, Department of Mineral Resources, Bangkok.

Khundee, K., Kererattanasathian, V., Hongsaban, N., Khlonkratoke, A., Maihom P., and Tewa, C., (2019). Coastal changes along the Petra Beach to Ao Noon Bay, La-ngu District, Satun Province. Environmental Geology Division, Department of Mineral Resources, Bangkok. 15 p.

Meesook, A. (2014). Lithostratigraphy, Faunal assemblages, Biodiversity, Paleocology and Environment of Deposition of the Cambrian-Permian Rocks in Satun Province, Peninsular Thailand, Technical report contract No. 39/2557, Bureau of Geological survey, Department of Mineral Resources.

Romana, M., 1985, New adjustment ratings for application of Bieniawski classification to slopes,in: Proceedings of the International Symposium on the Role of Rock Mechanics in Excavations for Mining and Civil Works. International Society of Rock Mechanics, Zacatecas, p.49-53

Sinsakul, S., 1988, Geological map of Amphoe Langu (4922 I) map sheet, scale 1:50,000, Department of Mineral Resources, Bangkok, Thailand.

Singh, B., Geol, R. K.2011, Engineering Rock Mass Classification, Tunneling, foundation, and landslides; Elsevier: New York

Sinsakul, S., Tiyapairach, S., Chaimanee, N., and Aramprayoon, B., 2002, Coastal change along the Andaman Sea coast of Thailand, Geological survey division, Department of Mineral Resources, Bangkok, 58p.

Thepju, W., Yamansabedean, N., & Bamrungsong, P., 2017. Karst features in Satun Geopark, Satun province. in DMR-CCOP-TNCU Technical Seminar on " Biostratigraphy and Karst Morphology of Satun Aspiring Geopark, 13-14 July 2017,The Berkeley, Hotel, Pratunam, Bangkok,Thailand, p.50-59.

Tiyapairach, S., 2004. Geological map of Ban Pak Bara (4922 IV) map sheet, scale 1:50,000, Department of Mineral Resources, Bangkok, Thailand.

Waltham, A.C., and Fookes, P.G. (2003). Engineering classification of karst ground conditions. Quarterly Journal of Engineering Geology and Hydrogeology.

Waltham, T., Bell, F. and Culshaw, M. (2005). Sinkholes and Subsidence, Karst and Cavernous Rocks in Engineering and Construction. Praxis Publishing, UK.

Wongvanish, T. (1990). Lithostratigraphy, sedimentology, and diagenesis of the Ordovician carbonates, Southern Thailand. University of Tasmania, unpublished Ph.D. thesis, 215 p.

If you are interested in earth sciences
Support geoscience with a subscription to

Thai Geoscience Journal

The **Thai Geoscience Journal** publishes original research
And review articles from the international community in all
Fields of geological sciences such as

Engineering Geology | Petrology | Geopark | Paleontology
Environmental Geology | Economic Geology | Structural Geology
Geophysics | Tectonics | Geochemistry

All articles published by the **Thai Geoscience Journal**
are made freely and permanently accessible online
Immediately upon publication, **without subscription charges or registration barriers.**

Contact
Geological Survey Division
Department of Mineral Resources 75/10 RAMA VI Road,
Ratchatewee, Bangkok 10400 Phone: +66(0)-2-621-9650
Website : https://www.dmr.go.th
E-mail : tgj.2020@gmail.com

Published by

CONCEPT DESIGN

This logo composes of Abbreviations of Thai Geoscience Journal

T = THAI G = GEOSCIENCE J = JOURNAL

Coexistence of 3 abbreviations design in a concept of modernity blend with a Thainess
Modification of G alphabet in a shape of ammonoid shows relevance to geology
and infinite development of Thai Geoscience Journal

- **SCOPE AND AIM OF THAI GEOSCIENCE JOURNAL (TGJ):** TGJ is an international (Thai and English) journal publishing original research articles dealing with the geological sciences. It focuses, mainly but not exclusively, on: Sedimentology and Geomorphology, Palaeontology, Quaternary, Geology and Environment Change, Geological Hazards, Environmental Geosciences, Geophysics, Mineral and Petroleum Geology, Tectonics and Structural Geology, Geochemistry and Geochronology, Metamorphic Geology and Volcanic and Igneous Geology. Two types of articles are published in the Journal: Research Articles and Reviews. Research Articles are new original articles, normally not exceeding 25 pages. Review Articles are those papers that summarize the current state of knowledge on specific fields or topics of geosciences. They analyze and discuss previously published research results, rather than report new results. TGJ Aim is to provide valuable geoscience knowledge and information and push more inspiration for readers and researchers to produce treasure research in the future.
- **FEEDBACK AND CONTACT:** We welcome your feedback, comments and suggestions for the development of TGJ

Please contact: Dr. Apsorn Sardsud (Editor-in-Chief, TGJ)
Department of Mineral Resources
75/10 RamaVI Road Ratchathewee Bangkok 10400, Thailand

Phone: +66 (0)2 6219650

Email: tgj.2020@gmail.com

Website: http://www.dmr.go.th

INSTRUCTIONS TO AUTHORS FOR TGJ

1. Submission of manuscripts.

The Thai Geoscience Journal (TGJ) is an international (Thai and English) journal publishing original research articles dealing with the geological sciences.

Two types of articles are published in the Journal: Research Articles and Reviews. Research Articles are new original articles. Review Articles are those papers that summarize the current state of knowledge on specific fields or topics of geosciences. They analyze and discuss previously published research results, rather than report new results. Copyright of all the contents of Thai Geoscience Journal belong to the Department of Mineral Resources in Thailand.

The manuscript should be sent to Editor in Chief via tgj.2020@gmail.com.

2. Requirement electronic file for submission.

1) The manuscript should be prepared in word and pdf files (download from https:// tgjdmr2019.wixsite.com/mysite)

2) Table file (word and pdf) must have a heading.

3) Figure file (JPEG, PNG, TIFF, EPS, PSD or AI) ; Resolution of all figures must be 300 – 600 dpi. Name of figure file should be related in manuscript.

3. Manuscripts Information.

The main document, containing cover sheet, main text, acknowledgement (if applicable), references, figure, table, figure and table captions.

Cover sheet: Cover sheet should contain 1) title, 2) full names and affiliations and the addresses of all authors 3) postal and e-mail addresses and phone and fax numbers of the Corresponding Author who will take responsibility for the proofs, and 4) running title composed of no more than 70 characters.

Title: A title is to be brief summarizes the major results of the paper.

Abstract: An abstract should be a condensation and concentration of the essential qualities of the paper. All papers, excluding Short Notes, are to be accompanied by an abstract not exceeding 500 words.

Key words: Select keywords (not more than six words or phrases) which identify the most important subjects covered by the paper and arrange them in alphabetical order.

Main text : Main text should contain Introduction ,Methods, Results, Discussions and Conclusions or something else as appropriate.

*Acknowledgements:*Brief acknowledgement of funding sources and assistance provided.

References: The references should be in a common citation format as shown below.

Figures and tables: Each figure and table must be mentioned sequentially in the text of the paper. Each figure must have a caption, and each table must have a heading. Captions and headings should be explicit enough that the reader can understand the significance of the illustration or table without reference to the text.

References

References in content, tables and images must specify author-date in-text citation, with the researcher's name followed by a comma (,) and the year of publication of the document behind the quote. If there are 1-3 researchers, specify the names of all the researchers But if there are more than 3 researchers, specify the first researcher and follow with et al.

Examples (Mogen, 2001), (Jones & Miler, 2008), (Mogen, Jones & Miler, 2008), (Halano et al. 2009)

Journals:

Barron, J.A.(1983). Latest Oligocene through early Middle Miocene diatom biostratigraphy of the eastern tropical Pacific. *Marine Micropaleontology,7,* 487−515.

Barron, J. A. and Keller, G. (1982). Widespread Miocene deep-sea hiatuses: Coincidence with periods of global cooling. *Geology, 10*, 577−581.

Nakamori, T. (1986). Community structures of Recent and Pleistocene hermatypic corals in the Ryukyu Islands, Japan. *Science Reports of the Tohoku University, 2nd Series (Geology), 56*, 71–133.

Zakharov, Yu. D. (1974). A new find of an ammonoid jaw apparatus. *Paleontologicheskii Zhurnal 1974*, 127−129. (in Russian; original title translated)

Book :

Ager, D. V. (1963). *Principles of Paleoecology*, 371 p. McGraw-Hill Co., New York.

Okuda, M., & Okuda, D.(1993). *Star Trek Chronology: The history of the future*. New York: Pocket Book.

Electronic material :

Japan Oceanographic Data Center, (2011), J-DOSS, Oceanographic Data and Information Download Service (Temperature, Current, Depth, Biology, Marine Information) [online]. [Cited 24 August 2011]. Available from: http://www.jodc.go.jp/index_j.html.

TGJ Contributors

Assoc. Prof. Dr. Apichet Boonsoong	Chiang Mai University, Thailand
Dr. Apsorn Sardsud	Department of Mineral Resources, Thailand
Prof. Dr. Che Aziz bin Ali	Universiti Kebangsaan Malaysia, Malaysia
Prof. Dr. Clive Burrett	Mahasarakham University, Thailand
Assoc. Prof. Dr. Danupon Tonnayopas	Prince of Songkla University, Thailand
Dr. Dhiti Tulyatid	Coordinating Committee for Geoscience Programmes in East and Southeast Asia (CCOP), Thailand
Dr. Ian Watkinson	University of London, England
Mr. Jittisak Premmanee	Department of Mineral Resources, Thailand
Prof. Dr. Katsumi Ueno	Fukuoka University, Japan
Prof. Dr. Katsuo Sashida	Mahidol University, Kanchanaburi campus, Thailand
Prof. Dr. Ken-Ichiro Hisada	University of Tsukuba, Japan
Assoc. Prof. Dr. Kieren Howard	Kingsborough Community College, City University of New York, USA
Prof. Dr. Koji Wakita	Yamaguchi University, Japan
Assoc. Prof. Dr. Kriengsak Srisuk	Khon Kaen University, Thailand
Assoc. Prof. Dr. Lindsay Zanno	North Carolina State University, USA
Dr. Mallika Nillorm	Department of Mineral Resources, Thailand
Dr. Martin Smith	Global Geoscience, British Geological Survey, UK
Adj. Prof. Dr. Michael Ryan King	Western Colorado University, Thailand
Prof. Dr. Montri Choowong	Chulalongkorn University, Thailand
Assoc. Prof. Dr. Mongkol Udchachon	Mahasarakham University, Thailand
Prof. Dr. Nigel C. Hughes	University of California, Riverside, USA
Mr. Niwat Boonnop	Department of Mineral Resources, Thailand
Asst. Prof. Nussara Surakotra	Khon Kaen University, Thailand
Asst. Prof. Dr. Passkorn Pananont	Kasetsart University, Thailand
Dr. Phumee Srisuwan	Department of Mineral Fuels, Thailand
Prof. Dr. Pitsanupong Kanjanapayont	Chulalongkorn University, Thailand
Dr. Pol Chaodumrong	Geological Society of Thailand, Thailand
Dr. Pradit Nulay	Department of Mineral Resources, Thailand
Dr. Prinya Putthapiban	Mahidol University Kanchanaburi Campus, Thailand
Prof. Dr. Punya Charusiri	Department of Mineral Resources, Thailand
Asst. Prof. Dr. Rattanaporn Hanta	Suranaree University of Technology, Thailand
Assoc.Prof. Rungruang Lertsirivorakul	Khon Kaen University, Thailand
Assoc. Prof. Dr. Sachiko Agematsu-Watanabe	University of Tsukuba, Japan
Dr. Sasiwimol Nawawitphisit	Department of Mineral Resources, Thailand
Dr. Seung-bae Lee	Korea Institute of Geoscience and Mineral Resources, Republic of Korea
Dr. Siriporn Soonpankhao	Department of Mineral Resources, Thailand
Asst. Prof. Dr. Sombat Yumuang	Geo-Informatics and Space technology Development Agency, Ministry of Science and Technology (GISTDA), Thailand
Mr. Somchai Chaisen	Department of Mineral Resources, Thailand
Dr. Surin Intayos	Burapha University, Chanthaburi Campus, Thailand
Mr. Sutee Chongautchariyakul	Department of Mineral Resources, Thailand
Dr. Tawatchai Chualaowanich	Department of Mineral Resources, Thailand
Mr. Thananchai Mahatthanachai	Department of Mineral Fuels, Thailand
Assoc. Prof. Dr.Thasinee Charoentitirat	Chulalongkorn University, Thailand
Dr. Toshihiro Uchida	Retired geophysicist, Japan
Mr.Tritip Suppasoonthornkul	Department of Mineral Fuels, Thailand
Dr. Weerachat Wiwegwin	Department of Mineral Resources, Thailand
Assoc. Prof. Dr. Yoshihito Kamata	University of Tsukuba, Japan
Dr.Andrew Mitchell	Consultant, Myanmar Precious Resources Group, Yangon, Myanmar
Dr. Jingwen SU	Nanjing Center, China Geological Survey, Nanjing, China
Dr. Songyang WU	Coordinating Committee for Geoscience Programmes in East and Southeast Asia (CCOP), Thailand
Dr.Apivut Veeravinantanakul	Mahidol University, Kanchanaburi campus, Thailand

Thai Geoscience Journal
Vol. 4 No. 6
July 2023
ISSN 2730-2695

CONTENTS

Published by
Department of Mineral Resources
Geological Society of Thailand
Coordinating Committee for Geoscience Programmes in East And Southeast Asia (CCOP)